Site-Directed Mutagenesis of Glutathione Transferase, GstB from *Escherichia coli* for Use in Bioremediation

By Nancy Rop Keter

Submitted in Partial Fulfillment of the Requirements

for the Degree of

Master of Science

in the

Chemistry

Program

YOUNGSTOWN STATE UNIVERSITY

May, 2021

Site-Directed Mutagenesis of Glutathione Transferase, GstB from *Escherichia coli* for Use in Bioremediation

Nancy Rop Keter

I hereby release this thesis to the public. I understand that this thesis will be made available from the OhioLINK ETD Center and the Maag Library Circulation Desk for public access. I also authorize the University or other individuals to make copies of this thesis as needed for scholarly research.

Signature:

_____

Nancy Rop Keter, Student Date

Approvals:

_____

Dr. Nina V Stourman, Thesis Advisor Date

_____

Dr. Jonathan Caguiat, Committee Member Date

_____

Dr. Michael Serra, Committee Member Date

_____

Dr. Salvatore A. Sanders, Dean of Graduate Studies Date

ABSTRACT

The problem of environmental pollution can be effectively solved by employing a good bioremediation strategy. Pollution caused by polyhalogenated wastes poses great danger to life and has been a problem of high concern globally. The project was aimed to take a step forward finding an effective solution to the problem of pollution by employing glutathione transferase enzymes that could be engineered to clean up contaminated sites.

Glutathione transferases (GSTs) are a superfamily of protective enzymes that function in the detoxification of endogenous and xenobiotic electrophiles by conjugating them with glutathione. Glutathione transferase B, GstB encoded by the *yliJ* gene and expressed in *E. coli* has been found to be able to catalyze the conjugation of small electrophilic substrates with glutathione converting these toxic compounds into less harmful hydrophilic byproducts.

Four mutant GstB enzymes R119A, R119S, R119Q and R119H were expressed, purified, and studied along with the wild type to determine the role of the amino acid residue at position 119 of GstB in dictating the binding of bromoacetate at the H-site. The kinetic parameters, k_{cat}, k_{cat}/K_M and Michaelis constant K_M, showed the significance of the amino acid residue at position 119 in the binding of bromoacetate at the H-site. Using site-directed mutagenesis two new mutants L114F and L114F/R119A, which are postulated to have an enlarged substrate binding pocket to accommodate bulky aromatic substrates, were created.

ACKNOWLEDGEMENT

First, I am very thankful to God for His help in everything, I could not have made it this far without His immense blessings. My sincere gratitude goes to my advisor Dr. Nina V Stourman, I will forever be grateful to her for her unending support and kindness while I was working in her lab, I cannot take it for granted that she went far and beyond to help in all ways, I count myself very lucky to have been in her lab, I have gained a lot of experience working with her. I admire her dedication and I highly appreciate the fact that she sacrificed a lot to help not only with my research, but also for her patience, she had to go through sleepless nights assisting in the preparation of my thesis. I am very thankful to Dr. Jonathan Caguiat and Dr. Michael Serra, for sacrificing their time to assist as my thesis committee members; I highly appreciate their patience reading and guiding with my thesis, given the short amount of time that was available between datelines. They were a blessing in the most difficult moment, and I will never forget their kindness. I truly appreciate the work Jennifer M. Moore and Collins Aboagye in building a solid foundation for the project and to Dr. Stourman's group members for their assistance in the lab.

I will forever be indebted to the Department of Chemistry for the opportunity they gave me and the financial help and moral support. Thanks to Dr. Lovelace-Cameron and to Dr. Timothy Wagner for the graduate assistantship and scholarship, they have truly transformed my life. I am sincerely thankful to Lisa Devore for her kindness and support in the department. I do not have enough words to express my gratitude to all the professors in the department and to the entire chemistry fraternity for their enormous support in my journey at YSU. I am very thankful to Dr. Salvatore A. Sanders and the Graduate School for giving me the opportunity to join YSU and for the financial aid, I could not have made it this far without their generous support. From the bottom of my heart, thank you all.

TABLE OF CONTENTS

LIST OF FIGURES

LIST OF TABLES

LIST OF ABBREVIATIONS

Abs	absorbance
AEC	anion exchange chromatography
BrAc	bromoacetic acid
BSP	sulfobromophthalein sodium
CDNB	1-chloro-2,4-dinitrobenzene
cGSTs	cytosolic glutathione transferases
Da	Dalton
DDE	1,1-dichloro-2,2-*bis(p*-chlorophenyl)ethylene
DDT	1,1,1-trichloro-2,2-bis [*p*-chlorophenyl]ethane
dNTP	deoxyribosenucleoside triphosphate
dsDNA	double stranded deoxyribonucleic acid
DTNB	5,5'-dithiobis(2-nitrobenzoic acid)
DTT	dithiothreitol
Ɛ	molar extinction coefficient
EBI	European bioinformatics institute
E. coli	*Escherichia coli*
EDTA	ethylenediaminetetraacetic acid
GS-acetate	glutathione acetate
GSH	glutathione
GST	glutathione transferase
IPTG	isopropyl-β-D-1-thiogalactopyranoside
LB	Luria-Bertani medium
MAPEG	Membrane Assisted Proteins in Eicosanoid and Glutathione Metabolism
OD_{600}	optical density at 600 nm
PCR	polymerase chain reaction
PDB	protein data bank
pI	isoelectric point
RNA	ribonucleic acid

rpm	revolutions per minute
SDS-PAGE	sodium dodecyl sulfate polyacrylamide gel electrophoresis
SOB	super optimal broth
SOC	super optimal broth with catabolite repression
T_m	melting temperature
WT	wild type

CHAPTER 1

1.0 INTRODUCTION

Environmental pollution is one of the major problems of high concern globally. Toxic chemicals find ways into the environment because of their use in several areas especially in agriculture and industry.[1] Polyhalogenated aromatic hydrocarbons (PHAHs), for instance, are one class of toxic compounds that are ingredients in many insecticides.[2] A good example of a compound in this class is 1,1,1-trichloro-2,2-bis [*p*-chlorophenyl]ethane, DDT (Figure 1), which was banned in the United States and Europe because of its toxicity and persistence in the environment.[1] Sadly, DDT is still being used in some other countries as an insecticide to kill mosquitos in the management of malaria .[2,3,]

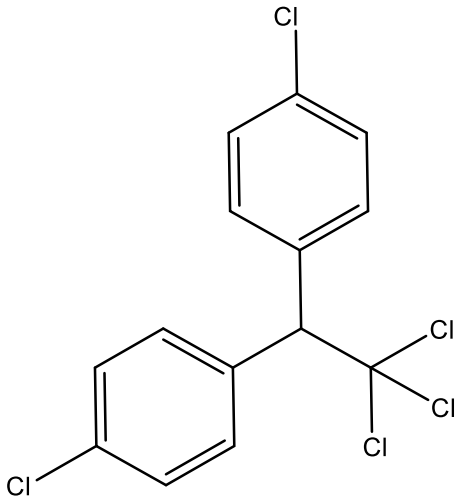

Figure 1: The structure of 1,1-trichloro-2,2-bis [p-chlorophenyl]ethane (DDT).

To deal with the problem of environmental pollution, bioremediation has been proposed as the best strategy to employ because of its safety, efficiency, and cost effectiveness. Bioremediation is the use of biological agents like microorganisms to break down toxic compounds with the aim of cleaning up a polluted environment .[3,4,5]

1.1 Glutathione Transferases and Glutathione

Glutathione transferases (GSTs) (Figure 2) are important enzymes that are present in many kingdoms of life including prokaryotes and eukaryotes. They work to detoxify endogenous electrophiles, which are usually formed because of oxidative stress, and xenobiotics like environmental pollutants. In prokaryotes, GSTs are highly expressed in bacteria like *E. coli* .[8.]

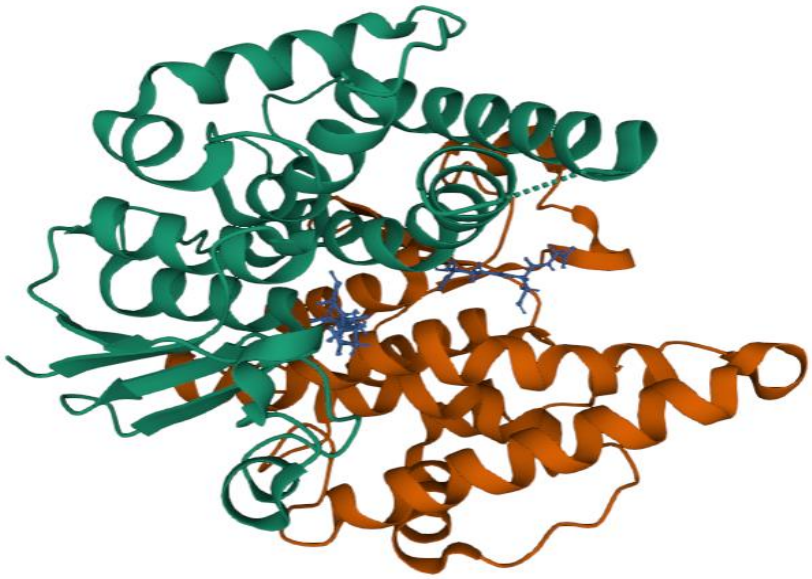

Figure 2: A crystal structure of a glutathione transferase from Salmonella enterica *with bound GSH, viewed in Mol* Viewer; PDB ID: 4KH7. The two subunits are colored in green and brown, while the two GSH substrates are colored in blue.* [21,26]

GSTs are dimeric proteins where each monomer has two active sites to accommodate two substrates. The H-site of these enzymes acts as the binding site for the electrophile and the G-site binds glutathione (GSH).[8,9]

Glutathione is an essential cofactor of glutathione transferase which participates in all the enzyme's detoxication processes. Glutathione is a molecule made up of three amino acids: glutamate, cysteine, and glycine (Figure 3). It has a special peptide bond between glutamate and cysteine formed by linking the γ-carboxyl group of glutamate to the amino group of cysteine. When glutathione is bound to the G-site of GST at physiological pH, its cysteine sulfhydryl group becomes deprotonated, and GSH is converted into a strong nucleophile which can attack the electrophile bound at the H-site of the GST.[6,7]

An example of a reaction catalyzed by glutathione transferase GstB is the detoxication of bromoacetate, a known genotoxic by-product of water treatment. The conjugation reaction with GSH forms GS-acetate and hydrogen bromide which are both less toxic hydrophilic products that can be easily eliminated (Figure 4).[9]

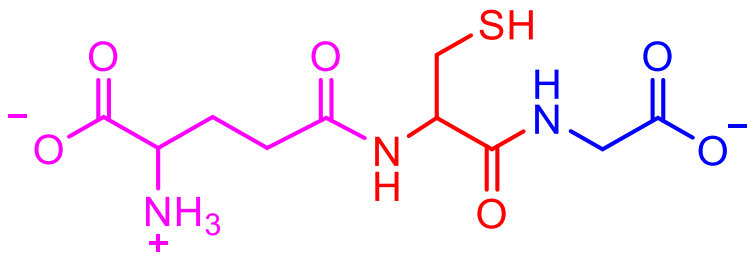

Figure 3: The structure of glutathione showing the three amino acids - glutamate, cysteine and glycine labelled in pink, red and blue colors, respectively.

1.2 Glutathione Transferase Discovery

Glutathione transferase was first discovered in 1961 and found to catalyze a reaction between GSH and 4-nitropyridine N-oxide or 4-nitroquinoline N-oxide, respectively.[10] In a study by Al-Kassab and colleagues,[11] a prepared homogenate from rat liver was observed to catalyze the conjugation of GSH and 3,4-dichloronitrobenzene resulting in the liberation of a chlorine from position 4 in the benzene ring. The study was able to show that during the catalyzed reactions, the chemical groups were displaced based on their reactivity ranking. The liver homogenate supernatant was also able to catalyze the conjugation of GSH to some polychloronitrobenzene substrates, liberating nitrate ions. From these results, an important observation was made that the ratio of GSH used in the reaction was directly proportional to the amount of nitrite ions liberated. Reactions with stable substrates like 2,4,5-trichloronitrobenzene did not proceed despite the presence of the enzyme and GSH; and when the enzyme and chloronitrobenzenes were incubated in the absence of GSH, no reaction was observed, demonstrating the valuable role of GSH in the reaction. [11]

In another study, the liver homogenate supernatant was able to catalyze the conjugation of sulfobromophthalein sodium (BSP) and GSH liberating bromide.[30] No activity was observed after boiling the liver at 100 °C, or when the enzyme and BSP were incubated without GSH. The significance of GSH in the reaction and the presence of a free sulfhydryl group were also shown to be crucial for successful conjugation since no reaction was recorded with oxidized GSH. It was also observed that the thiolate group from GSH could displace the bromide group of BSP, thus occupying its position on the benzene ring. [30]

1.3 Classification of Glutathione Transferases

Canonical glutathione transferases have been grouped into cytosolic, kappa class enzymes (mitochondrial), bacterial fosfomycin resistance proteins, and microsomal (MAPEG) super families.[8,12,13,22,23] The classification is based on their molecular structure and their physical and chemical properties. As a rule, the GSTs are grouped according to their sequence similarity, where those GSTs that bear 40% or higher identity assigned to the same class, if the sequence identity is below 25%, they are grouped separately.[8]

The largest super family comprising the cytosolic GSTs has been subdivided into two sub-families: one for mammals and another for non-mammalian species. [12,13] The first seven classes set for the mammals include the *alpha, mu, pi, sigma, theta, omega*, and *zeta* class, while other classes like the *beta, chi, delta, epsilon, lambda, phi,* and *tau* are predominantly set for non-mammalian species. The *epsilon* and *delta* classes are specific to only the insects and have been highly associated with resistance to insecticides like organochlorides, organophosphates, and pyrethroids.[8,12] Many cytosolic GSTs work by conjugating electrophilic substrates with glutathione and offer protection against free radicals. They are homodimeric proteins with a total molecular weight of approximately 50 kDa. [8,12,13,22]

The bacterial cytosolic glutathione transferases (cGSTs) have also been divided into several classes based on their structural and functional properties. The five known classes include the *beta, chi, theta, nu,* and *zeta*.[8] The bacterial *theta* class shares some unique characteristics with the other non-human *theta* class cGSTs, which include their amino acid sequence, their inability to bind to a glutathione column as well as their poor catalytic efficiency with substrates like 1-chloro-2,4-dinitrobenzene (CDNB). The *beta*

class is a special class among the bacterial cGST that has been isolated and purified from many bacterial species. This class is not only identified by its unique binding affinity to a glutathione column but also because of its G-site bearing cysteine groups. Examples of a GSTs from the beta class are the *EcGST* isolated from *E. coli,* OaGST from *Ochrobactrum anthropi* and BxGST/ BphK from *Burkholderia xenovorans*.[8,12,13]

Bacteria have many GST genes with diverse sequences whose functions have not yet been studied. Six homologous genes have been identified in *E. coli* bacteria, and two of these genes, *yfcf* and *yfcg*, are thought to be responsible for protecting the bacteria from oxidative radicals.[8,24, 25,27.] The *E. coli* bacteria is also known to have a beta class GST, a stringent starvation protein A (SspA), as well as an RNA polymerase with close resemblance in fold to that of cGSTs.[8]

Although many GSTs perform the important work of detoxication in organisms, the different classes of GSTs may differ in their molecular structure.[8.] The differences in the structure contribute in dictating the binding affinities of a variety of substrates to the enzymes. Unlike some insect GSTs which have been observed to metabolize aromatic electrophilic substrates like DDT, most bacterial GSTs have not shown any significant activity towards such bulky substrates [8,16,17]

1.4 Bromoacetate -glutathione conjugation by Glutathione Transferase *GstB*

Glutathione transferase GstB has been shown to catalyze the conjugation of GSH to small electrophilic molecules like bromoacetate (Figure 4). [9]

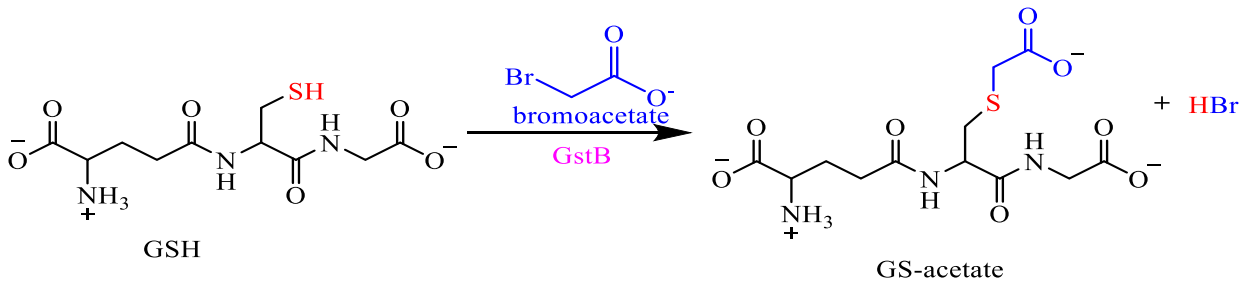

Figure 4: Detoxication of bromoacetate by conjugation with glutathione (GSH) catalyzed by a GstB enzyme. [9]

Desai and Miller worked to find out how bacteria can survive in an environment surrounded by toxicants like bromoacetate, so they studied a library of *E. coli* strains with a single gene mutation.[9] The journey led them to a discovery of *yliJ* as a gene in *E. coli* that encodes glutathione transferase B (*GstB*), an enzyme responsible for detoxification of xenobiotics like bromoacetate. The scientists were able to express, purify, and study the kinetic properties of the enzyme. Interestingly, they found that GstB can greatly enhance the rate of conjugation of bromoacetate to GSH, proceeding at a rate which was five times faster than the uncatalyzed rate. Analysis of data using a Michaelis - Menten plot gave a turnover number (k_{cat}) of 27 s^{-1}, which represented the number of substrates that each enzyme's active site could convert into products in a second; while Michaelis constant (K_M), for bromoacetate was obtained as 5 mM, meaning that half of the active sites were occupied, when the concentration of bromoacetate was 5 mM. [9]

1.5 Identification of Important Amino Acid Residues for Activity of GstB

Chrysostomou and coworkers were able to study the H-binding site of GstB to see which amino acid residues are responsible for positioning electrophilic substrates at the H-site closer to GSH.[14] Three arginine (R) residues at position 7, 111 and 119 of GstB, located

7Å closer to the GSH binding site are conserved, and thus suspected to contribute to GSH binding and positioning of electrophilic substrates closer to glutathione.

To study the role of the arginine residues, a mutation was done to substitute the amino acids with glutamine to form R119Q and a R111Q/R119Q mutants. A study of the enzymes indicated that the activity of R119Q towards many electrophilic substrates including bromoacetate was significantly decreased, while the R111Q/R119Q experienced a total loss of activity.

A conclusion was therefore made that arginine residues at positions 111 and 119 of GstB are responsible in positioning electrophilic substrates bound at the H-site closer to glutathione. In addition, the amino acid residues may also be responsible for attracting substrates at the active site of the GstB enzyme.

A likely explanation for the loss of activity of GstB is that the mutations might have negatively influenced the expression or stability of the enzyme, but upon further analysis it was later concluded that the arginine residues may be responsible for activation of the thiolate group of glutathione as well as also contributing to binding of electrophilic substrates at the H-site.

1.6 Expanding the Substrate Specificity of GSTs

The relationship of an enzyme with substrate is dictated by many factors, one being the specificity of the substrate binding pocket. Affinity of substrates for the active site can be modulated by altering the substrate binding site residues to favor the binding or by creating enough space in the binding pocket for the substrate to fit in. Few scientists have

tried to study and modify the H-binding site of GSTs to increase the affinity and catalytic efficiency of the enzymes to common environmental pollutants as potential substrates.

Site-directed mutagenesis can be used to study the interaction of enzymes with substrates. A study of *Burkholderia xenovorans LB400 (BphK^{LB400})* GST was done by McGuinness and reported in 2007.[15] Site-directed mutagenesis was performed to generate mutants of *BphK^{LB400}* GST with the aim of modulating its substrate specificity to accommodate chlorinated organic toxicants. Using a *bphK* gene in the *Burkholderia xenovorans LB400* stain, the group generated a GST mutant by substitution of alanine at position 180 with proline to form A180P. A study of the interaction of the GST mutant with the model substrate, 1-chloro-2,4- dinitrobenzene, revealed an increase in activity of the A180P mutant compared to wild type. The de-chlorination reaction involving toxic substates like N-(3-chloro-4-methylphenyl)-2-methylpentanamide (Pentanochlor) and 2-chloro-N,N,N-trimethylethanaminium chloride (Chlormequat chloride) showed the activity of the mutant enzyme to have increased by 1.4 fold and 1.2 fold with regard to Pentanochlor and Chlormequat chloride substrates, respectively.[15] A conclusion was hence made that the A180P mutation was important in dictating the substrate specificity of the GST.

In some others studies, the *Anopheles funestus* glutathione transferase, *GSTe2* (*epsilon* class GSTs) was observed to catalyze the conversion of DDT into less toxic by-products.[16,17] Due to overuse of DDT to control mosquitoes in some parts of Africa, resistance was recorded in these insects and *GSTe2* was shown to be involved in the resistance.[16] Insights into the molecular structure of the detoxication enzymes involved in conferring the resistance to such harmful compounds can provide a lasting solution in the environmental remediation field.

To find the cause of resistance to DDT by mosquitos, Riveron and colleagues[16] studied the role of *GSTe2* from *Anopheles funestus* in the insecticide resistance. A crystal structure of the enzyme was analyzed, and the results revealed a mutation in *GSTe2* where leucine (L) 119 was substituted with an aromatic amino acid, phenylalanine (F) yielding the L119F mutant. The mutation was postulated to have played a significant role in enlarging the size of the binding pocket to accommodate the bulky hydrophobic DDT and creating an easy entry of the substrate into the active site.[16] It was observed in the crystal structure that binding of DDT at the N- terminus of *GSTe2* could have occurred due to an inclination of the C- terminal in part of the helix (Figure 5B) triggered by the L119F mutation within the helix.[16] The distortion of the helix played an important role in enlarging the substrate binding pocket to accommodate the bulky DDT (Figure 5C).

Wang and colleagues reported that the inclination of the helix shifted three important residues: alanine-112, glycine-116, and phenylalanine-120 to a closer proximity to glutathione.[17] The aromatic amino acid residue, F119 was believed to form a hydrophobic 'pocket cap' in the putative DDT binding pocket thus increasing the affinity of the enzyme to DDT. A closer analysis of the *GSTe2* structure with bound glutathione indicated a possibility of DDT being converted to 1,1-dichloro-2,2-*bis(p*-chlorophenyl)ethylene (*p,p'*-DDE) via an elimination reaction.[17] When glutathione is activated, its nucleophilic thiolate group can attack DDT at the beta hydrogen, resulting in the formation of 1-dichloro-2,2-*bis(p*-chlorophenyl)ethylene and HCl (Figure.6).

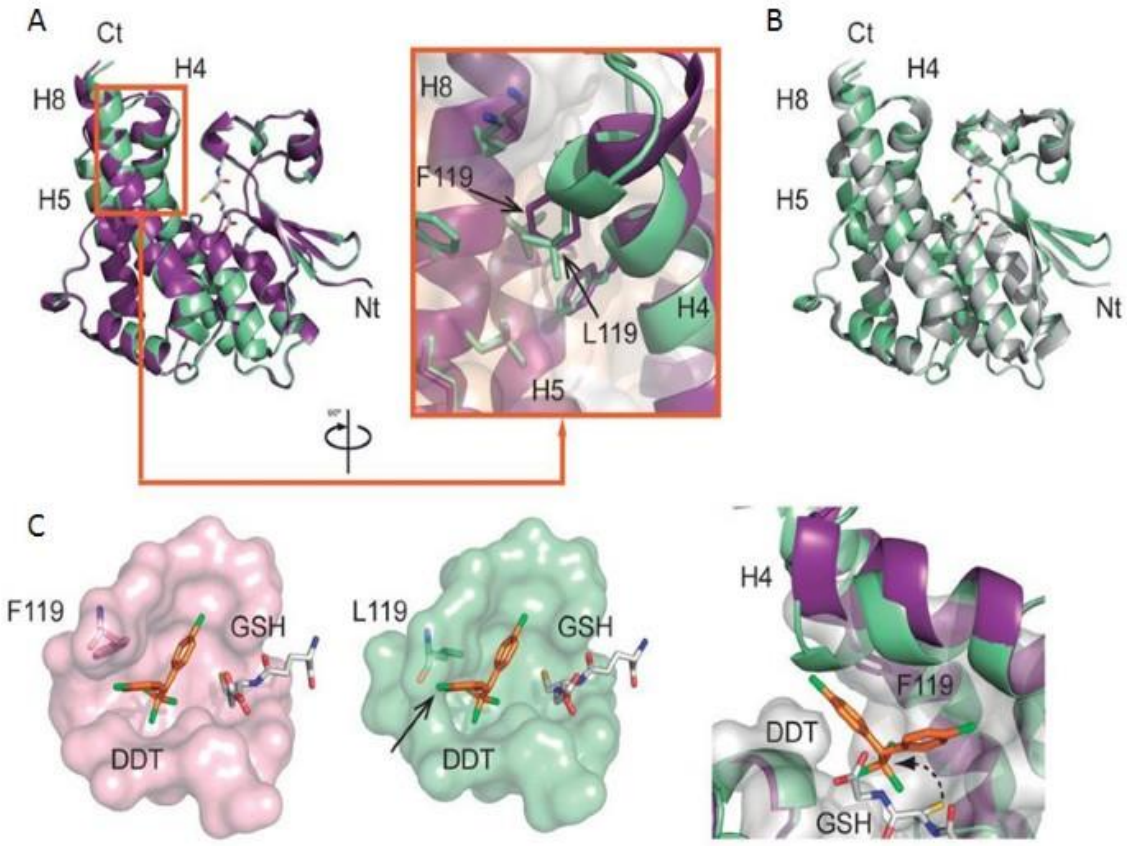

Figure 5: Images of wildtype and mutant GSTe2, extracted from Genome biology[16], showing the effect of the L119F mutation in GSTe2 detoxication of DDT. A) A superimposed image of mutant and wildtype GSTe2, used to compare the effect of the mutation on the structure of GSTE2; the purple represents the mutant enzyme while the green represents the wildtype; (B) shows the inclination of helix4 bearing the L119F mutation which distorts the helix enlarging the size of the substrate binding pocket to fit DDT; (C) the size of the substrate binding pocket is enlarged in the mutant (pink) and narrow in wildtype (green).

The numerous unsuccessful attempts to co-crystalize *apo-agGSTe2* bound to the substrate, DDT, suggested that the activity of GSTe2 is highly dependent on the participation of its cofactor, glutathione.

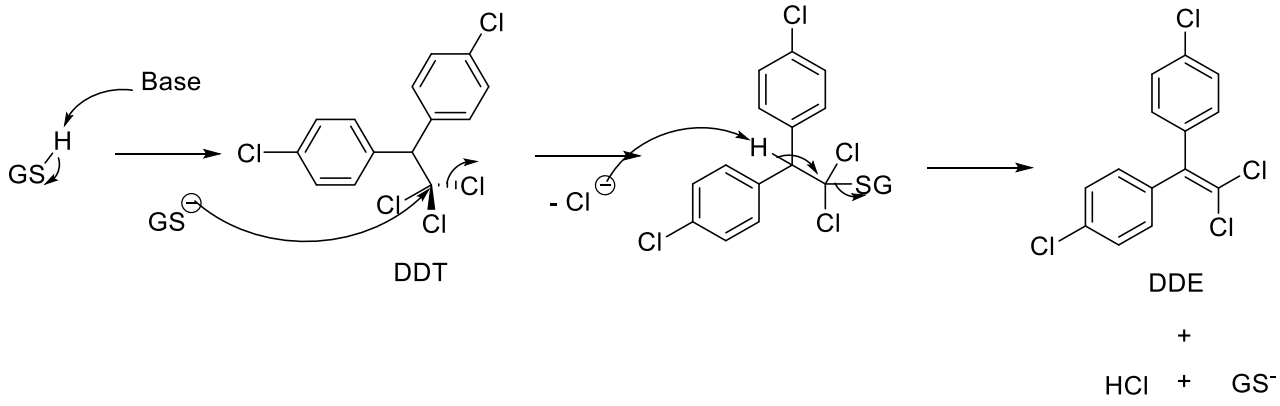

Figure 6: An elimination reaction that converts 1,1,1-trichloro-2,2-bis [p-chlorophenyl] ethane DDT) to 1,1-dichloro-2,2-bis(p-chlorophenyl)ethylene (p,p'-DDE), while GSH is converted to its nucleophilic form, GS^-.[17]

The study of Riveron and colleagues underscored the important role of the L119F mutation that introduced a hydrophobic aromatic residue, phenylalanine, in the putative H-binding site of the GST effectively enlarging the size of the substrate binding pocket of the enzyme. It is evident that such mutations can play a significant role in the alteration of an enzyme's substrate specificity.

1.7 Previous Work

Collins Aboagye and Jennifer Moore, both former graduate students in Dr. Stourman's laboratory, worked to build the pillar of the GstB project. Aboagye was able to express and purify GstB from *E. coli*. He also developed an effective method of testing the wildtype enzyme activity.[19] Continuing the project, Moore improved the method of analysis and created four mutants of GstB; R119H, R119S, R119Q, and R119A. [18] She used a discontinuous spectrophotometric assay to study the kinetic properties of the proteins and was able to show that the modification of amino acids located at the GstB active site can affect the specificity of substrate binding of the enzyme; however, the proteins were not fully characterized.

1.8 Research Problem and Objectives

Environmental pollution has been a huge burden of global concern. Since the industrial revolution, many toxic compounds are overflowing in the environment posing numerous effects on living organisms. It is therefore crucial for intensive study to be directed towards effective pollution management strategies.

In support of the proposal to employ bioremediation in environmental cleaning, this research was aimed at studying a GST enzyme for its potential in environmental remediation. [3,4,5] Site-directed mutagenesis was used to engineer a GstB mutant by substituting a branched-chained amino acid residue, leucine 114 with an aromatic amino acid residue, phenylalanine (F) resulting in L114F mutant. Another mutant was also engineered from an existing mutant (R119A) by substituting phenylalanine (F) for leucine (L) at position 114, resulting in a L114F/ R119A double mutant. The mutants were projected to be effective in catalyzing the conjugation of GSH to electrophilic substrates like the halogenated aromatic hydrocarbons.

Guided by the crystal structure of GstB from *Salmonella enterica* (PDB 4KH7), which has 83% sequence identity with the *E. coli* GstB (Figure 9), leucine at position 114 was seen to lie on the putative electrophile binding H-site located in the C-terminal (Figure 8) [14,20,21].

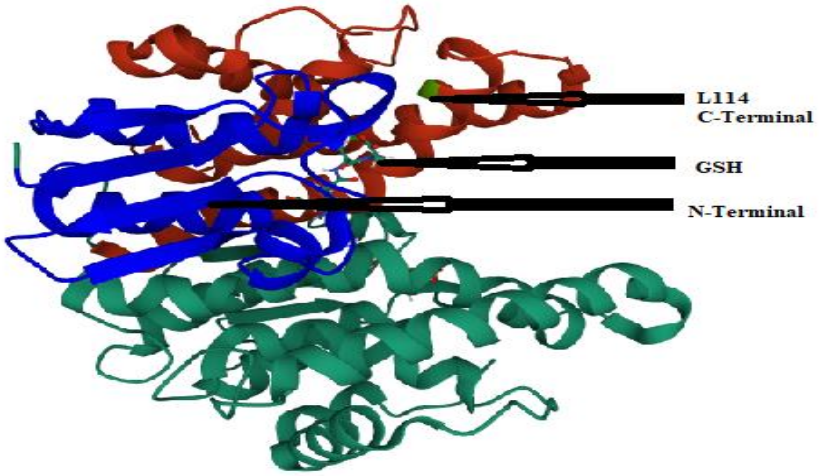

Figure 7: A 3D structure of glutathione transferase from S. enterica with bound GSH. Leucine 114 (light green) is positioned in the electrophile binding H-site, located in the C-terminal. PDB ID: 4KH7.[20,21]

```
S.enterica-GstB     MITLWGRNNSTNVKKVLWTLEELELPYDQILAGGKFGVNQDADYLAMNPNGLVPLLKDDE   60
E.coli-GstB         MITLWGRNNSTNVKKVLLTLEELELPYEQILAGREFGINHDADFLAMNPNGLVPLLRDDE   60
                    ********************.*********.*****.:**:*:***:************.***

S.enterica-GstB     TDLLLWESNAIVRYLAAQYGQNRLWVDNPARRAEGEKWMDWANQTLSPAHRVILWGLVRT   120
E.coli-GstB         SDLILWESNAIVRYLAAQYGQKRLWIDSPARRAEAEKWMDWANQTLSNAHRGILWGLVRT   120
                    :**:*****************:***:*.******.*********** *** ********

S.enterica-GstB     PPEKRDQAAIEAGIEKCDGLFALLDDALAHQPWFSGDNFGTGDIAIAPFVYNLLNVDLKW   180
E.coli-GstB         PPEERDQAAIDASCKECDALFALLDAELAKVKWFSGDEFGVGDIAIAPFIYNLFNVGLTW   180
                    ***.******:*. .::**.******  **:  *****:**.********:***:**.*.*

S.enterica-GstB     TPRPNLERWYQQLTERPAFRKVVMIPVT   208
E.coli-GstB         TPRPNLQRWYQQLTERPAVRKVVMIPVS   208
                    ******.***********.********:
```

Figure 8: A sequence alignment comparing the sequences of Escherichia coli glutathione transferase B with that of Salmonella enterica, done using the EBI Clustal Omega alignment tool.

A hypothesis was formulated that a mutation created by introducing phenylalanine at

GstB at the H- site may serve to enlarge the size of the binding pocket to accommodate

bulky aromatic substrates. Leucine is a branched chained amino acid residue, thus its substitution with phenylalanine (aromatic residue) in the putative substrate binding site may encourage a tighter interaction with the aromatic electrophilic substrates like DDT.

Since the mutants created by Moore were not fully characterized, the second objective of the project was to test the activity of the enzymes against both GSH and bromoacetate.

CHAPTER 2: MATERIALS & METHODS

2.1 Materials

Frozen DH5α cells, *E. coli BL21 (DE3)- pET20-gstB* cells and 4 mutants; *E. coli BL21 (DE3)- pET20-gstB R119A*, *E. coli BL21 (DE3)- pET20-gstB R119S*, *E. coli BL21 (DE3)- pET20-gstB R119Q* and *E. coli BL21 (DE3)- pET20-gstB R119H* were provided by Dr. Stourman. Luria-Bertani (LB) medium, SOB medium, isopropyl-β-D-1-thiogalactopyranoside (IPTG), ampicillin sodium salt, DL-dithiothreitol (DTT), ethylenediaminetetraacetic acid (EDTA), ammonium sulfate, streptomycin sulfate, anhydrous sodium phosphate monobasic, anhydrous sodium phosphate dibasic, Tris, Tris-HCl, glycerol, sodium chloride, sodium dodecyl sulfate (SDS) and N, N,N'N'-tetramethylethylenediamine (TEMED) were all purchased from Amresco (Solon, Ohio). The Q-Sepharose was purchased from GE Healthcare (Piscataway, NJ). The Coomassie Brilliant Blue R-250 staining solution was purchased from Bio-Rad (Hercules, CA), while Page Ruler unstained protein ladder and 40% Acrylamide were purchased from Thermo Fisher Scientific (Waltham, MA).

For site-directed mutagenesis, the following materials were obtained; Quick-change II Site-directed Mutagenesis Kit from Agilent Technologies (Santa Clara, CA), DNA oligonucleotide primers from Thermo Fisher Scientific (Waltham, MA), and QIAprep Spin Miniprep Kit from Qiagen (Germantown, MD).

For activity assay: Bromoacetic acid was purchased from Acros Organics (Belgium, NV) reduced L-glutathione, 5,5'-dithio-bis(2-nitrobenzoic acid) (DTNB), and 1-chloro-2,4-dinitrobenzene (CDNB) were all purchased from Sigma-Aldrich (St. Louis, MO).

All spectrophotometric assays were done using an HP Agilent 8453 Diode Array spectrophotometer purchased from Agilent Technologies (Santa Clara, CA).

2.2 Methods

2.2.1 Purification of Wild Type Expression and GstB and Mutants

BL21(DE3) cells containing *pET20 gstB* or the mutant gene initially stored as glycerol stock at -80 ^{o}C were used for protein purification. The same procedure was repeated for wild type and mutant proteins. The cells were inoculated in 50 mL Luria Bertani (LB) medium supplemented with 100 µg/mL of ampicillin and incubated overnight at 37 ^{o}C with shaking at 180 rpm. The cells were then diluted in a ratio of 1:100 in three large flasks, each containing 1.2 L of fresh LB media and 100 µg/mL ampicillin. Incubation was done with shaking at 180 rpm at 37 ^{o}C until an OD_{600} of 0.6 to 1.0 was attained. Isopropyl-β-D-1-thiogalactopyranoside (IPTG) was then added to a final concentration of 0.30 mM to induce protein expression. The cells were incubated overnight at 37 ^{o}C with shaking at 180 rpm. The cells were harvested by centrifugation at 6,000 x g for 10 min with temperature set at 4 ^{o}C to separate the cells from media. The resulting pelleted cells were frozen at - 20 ^{o}C. The frozen cells were then resuspended in a minimum amount of 20 mM Tris buffer, pH 7 containing 2 mM EDTA, 1 mM DDT and subjected to 12 cycles of sonication of 30 s each with 1 min intervals stirring on ice using a stirring plate.

A) Ammonium Sulfate Precipitation

After sonication, centrifugation was done at 11,000 x g for 20 min at 4 ^{o}C to separate the cell debris. To the supernatant, streptomycin solution was added dropwise to final concentration of 1% (w/v) to precipitate out the DNA, followed by centrifugation at 11,000 x g for 20 min at 4 ^{o}C. This was followed by the addition of ammonium sulfate to

the supernatant at 75% saturation to precipitate the protein. A final round of centrifugation was then done at 11,000 x g for 20 min at 4 ^{o}C. The supernatant was discarded while the pellet was kept and dissolved in a minimum amount of 20 mM Tris buffer, pH 7 containing 2 mM EDTA and 1 mM DDT. The dissolved protein sample was carefully transferred into the dialysis bag. The content was then left to dialyze overnight against 2 L dialysis buffer containing 20 mM Tris, 2 mM EDTA, 1 mM DDT, pH 7, in the cold room, on a magnetic stir plate with moderate stirring. Dialysis was repeated two times.

B) Anion Exchange Chromatography

A Q-Sepharose Fast Flow anion exchange column (3 x 12 cm) was equilibrated with 500 mL of 20 mM Tris buffer, pH 7, containing 1 mM DTT. Following dialysis, the volume of the protein which was measured to be approximately 10 mL for GstB (or mutant), was loaded onto the column and flow through was collected. The column was washed with 400 mL of 20 mM Tris, pH 7 buffer containing 1 mM DTT to elute unbound proteins. Finally, the bound proteins were eluted with 400 mL of 0 - 400 mM NaCl salt gradient in 20 mM Tris, pH 7.0, containing 1 mM DTT and fractions were collected using Bio-Rad 2110 fraction collector that was set to collect fractions at 3 minutes intervals.

C) Validation of GstB (or Mutant) Protein Presence

Collected fractions were stored in the cold room at 4 ^{o}C before being analyzed for the presence of protein by measuring the absorbance at 280 nm. The fractions that had absorbance of 0.7 AU or greater at 280 nm were subjected to 12.5% sodium dodecyl

sulfate–polyacrylamide gel electrophoresis (SDS-PAGE) to validate for the presence of the protein of interest.

Finally, the fractions containing sufficiently pure GstB protein were identified based on the results from SDS-PAGE. The fractions were combined and concentrated using the Amicon Ultra centrifugal filter units with a 10,000 Da, molecular weight cut off.

2.2.2 Activity Screening of GstB Mutants

A) Testing GstB and Its Mutants for Activity with Varying Bromoacetate Concentration

A discontinuous kinetic assay was performed. First, a quartz cuvette containing 925 µL of 200 mM Tris pH 8.0 and 50 µL of 5 mM of 5,5'-dithio-bis-(2-nitrobenzoic acid) (DTNB) in ethanol was used to blank the spectrophotometer at 412 nm before adding 25 µL of the reaction mixture. The absorbance was then taken at the 412 nm since one of the products of the reaction is 2-nitro-5-thiobenzoate anion (TNB^{2-}) which absorbs light at 412 nm.

Stock solutions of reagents were prepared and stored. First, a 50 mM stock solution of glutathione (GSH) was prepared and stored at –20 ^{o}C. A 146 mM stock solution of bromoacetate (BrAc) and 5 mM DTNB were prepared. GSH was prepared by dissolving solid GSH in 50 mM NaP_i, pH 7.0, and the final pH was adjusted to 7. Bromoacetic acid was prepared by dissolving bromoacetate crystals in 50 mM NaP_i, pH 7.0, and the final pH was adjusted to 7. To prepare DTNB, solid DTNB powder was dissolved in 100% ethanol.

For every uncatalyzed reaction, 360 µL of 50 mM NaP_i, pH 7.0 and 50 µL of 50 mM GSH were mixed well in a small tube before adding 90 µL of bromoacetate. The reaction was left to incubate for 2 minutes at room temperature. After the incubation period, a 25-

µL aliquot of the reaction mixture was added to a cuvette containing DTNB solution and the absorbance was taken at 412 nm. The procedure was repeated three times for each concentration of bromoacetate used, after which the mean was calculated. The concentration of bromoacetate in the reaction was varied from 1.6 mM to 26 mM.

For every catalyzed reaction, 350 µL of 50 mM NaP_i, pH 7.0, 50 µL of 50 mM GSH and 10 µL of 69 µM GstB (or mutant protein) was added to a cuvette and mixed well in a small tube before adding 90 µL of bromoacetate. The reaction was left to incubate for 2 minutes at room temperature. After the incubation period, a 25-µL aliquot of reaction mixture was added to a cuvette containing DTNB solution and the absorbance was taken at 412 nm. The concentration of bromoacetate was varied from 1.6 mM to 26 mM. All reactions were done in triplicate.

To calculate the rate of reaction, the concentration of GSH remaining after the spontaneous reaction (uncatalyzed) was subtracted from the concentration of GSH remaining at the end of the catalyzed reaction and the value obtained was divided by the reaction time. The Equation 2-1 below was used to calculate the concentration of GSH remaining after each reaction.

Equation 2-1.

$$c = \frac{A_{412}}{\varepsilon l} \text{ x } \mathbf{DF} \text{ x } \frac{1000\ mM}{1\ M}$$

where: c- concentration (mM); ε - extinction coefficient (13,600 L mol^{-1} cm^{-1}); l - path length (cm); DF- dilution factor

B) Testing GstB and Its Mutants for Activity with Varying Glutathione Concentration

A discontinuous kinetic assay was done by measuring the absorbance at 412 nm. First, a cuvette containing 925 µL of 200 mM Tris pH 8.0 and 50 µL of 5 mM of DTNB in ethanol was used to blank the spectrophotometer at 412 nm before adding 25 µL of the reaction mixture. Serial dilution was used to prepare several solutions of GSH of various concentrations and titrated as controls to ensure that the concentration of GSH was between 1.5 mM and 30 mM. Each control consisted of 50 µL of GSH diluted in 450 µL of 50 mM NaP_i, pH 7.0. From each control tube, a 25 µL aliquot was transferred to a cuvette containing 925 µL of 200 mM Tris pH 8.0 and 50 µL of 5 mM DTNB in ethanol. Absorbance was taken at 412 nm and the procedure was repeated three times. The mean value of absorbance was used to calculate the concentrations of GSH for each dilution according to Equation 2-1 above.

For every uncatalyzed reaction, 360 µL of 50 mM NaP_i, pH 7.0 and 50 µL of GSH were mixed before adding 90 µL of 100 mM bromoacetate. The reaction was left to incubate for 2 minutes at room temperature. After the incubation period, a 25 µL aliquot of reaction mixture was added to a cuvette containing DTNB solution and absorbance was taken at 412 nm. The concentration of GSH in the reaction was varied from 1.5 mM to 30 mM. All the reactions were performed in triplicate.

For every catalyzed reaction, 350 µL of 50 mM NaP_i, pH 7.0, 10 µL of GstB (or mutant) was added (1.4 µM in reaction), and 50 µL of GSH was added to the reaction tube and mixed before adding 90 µL of 100 mM bromoacetate. The reaction was left to incubate for 2 minutes at room temperature. After the incubation period, a 25 µL aliquot of reaction mixture was added to a cuvette containing DTNB solution and the absorbance

was taken at 412 nm. The concentration of GSH in the reaction was varied from 1.5 mM to 30 mM. All the reactions were performed in triplicate.

To calculate the rate of reaction, the concentration of GSH remaining after the spontaneous reaction (uncatalyzed) was subtracted from the concentration of GSH remaining at the end of the catalyzed reaction and the value obtained was divided by the reaction time. The concentration of GSH remaining after each reaction was calculated using **Equation 2-1**.

For each assay done with varying bromoacetate and GSH concentrations, the rate of reaction was calculated, and data obtained was fitted to a Michaelis-Menten model accounting for substrate inhibition (**Equation 2-2**) and the inhibition constant (K_i) was also determined in the model using **Equation 2-3** below.

Equation 2-2 $$\nu_0 = \frac{Vmax[S]}{[KM]+[S]\left(1+\frac{[S]}{Ki}\right)}$$

Equation 2-3: $$y = \frac{Vmax}{\left(\frac{x+KM}{x}+\frac{x}{Ki}\right)}$$

where: ν_0 *= initial velocity;* V_{max}*= maximum velocity;* K_M *= Michaelis constant; [S] = concentration of substrate;* K_i*= the inhibition constant.*

The kinetic parameters: K_i, V_{max}, *and* K_M were determined by adjusting the value of R^2, the coefficient of determination, to as close to 1.0 value as possible. The k_{cat} was calculated by dividing the value of V_{max} by the total concentration of enzyme used.

2.2.3 Site-directed Mutagenesis

A) Primer Design

The primers for L114F and L114F/R119A double mutant were designed and sent to Invitrogen to be synthesized. The primers were designed to be between 25 to 45 bases in length and to contain the desired mutation, according to the mutagenic primer design protocol. For L114F, the primer had an introduced mutation in which the CTG codon for leucine (L) was replaced with a TTT codon for phenylalanine (F); while the L114F/R119A double mutant had two-point mutations where the CTG codon for L was substituted with a codon TTT for F and an AGA codon for arginine (R), exchanged with a GCA codon for alanine (A), as underlined in the primers below.

Forward primer L114F: 5'-gctcatcgcgggatc**ttt**atgggattagtcagaacac-3'

Reverse primer L114F: 5'-gtgttctgactaatcccat**aaa**gatcccgcgatgagc-3'

Forward primer L114F, R119A: 5'-gctcatcgcgggatc**ttt**atgggattagtc**gca**acac-3'

Reverse primer L114F, R119A: 5'- gtgt**tgc**gactaatcccat**aaa**gatcccgcgatgagc-3'

Calculations of primers melting temperature, T_m

The melting temperature (T_m) of the primers was calculated to meet the requirement of the protocol demanding the T_m to be greater than or equal to 78 ^oC. The T_m was calculated according to **Equation 2-4** below.

Equation 2-4: Tm= $81.5 + 0.41(\%GC) - \frac{695}{N} - \%\,mismatch$;

where: N is the primer length in bases, % GC and % mismatch are rounded to whole numbers

B) Plasmid Purification

A 3-mL aliquot of liquid LB containing 100 μg/mL ampicillin was prepared in two separate sterile culture tubes. Using a sterile toothpick, a small number of cells were obtained from frozen glycerol stock of the *E. coli BL21(DE3)-pET20b-gstB* cells and *E. coli BL21(DE3)-pET20b-gstB R119A* glycerol stock cells were inoculated in the two tubes, respectively. The cells were then left to incubate overnight at 37 ^{o}C with shaking at 200 rpm.

Plasmids were purified using QIAprep Spin Miniprep Kit following the manufacturer protocol. A 1-mL aliquot of the overnight bacterial culture was placed in two separate labelled Eppendorf tubes and centrifuged for 1 minute at 13,000 rpm. The supernatant was discarded, and another 1-mL aliquot of the respective bacterial culture was added to the same tube and centrifuged for 1 minute at 13,000 rpm. The supernatant was discarded from each tube, and the bacterial cells pellet were resuspended in 250 μL of P1 buffer and mixed thoroughly by gentle pipetting of the solution up and down. A 250 μL aliquot of P2 buffer was added and immediately mixed thoroughly by gentle inversion of the tubes 6 times. Lastly, 350 μL of N3 buffer was also added and immediately mixed thoroughly by gentle inversion of the tubes 6 times, followed by centrifugation at 13,000 rpm for 10 minutes in a microcentrifuge.

The supernatant was applied to a QIAprep spin column by pipetting and centrifuged at 13,000 rpm for 60 seconds after which the flow-through was discarded. The column was washed with 500 μL of PB buffer and centrifuged 60 seconds before discarding the flow-through. A second wash of the column was repeated using 750 μL of PE buffer, followed

by centrifugation at 13,000 rpm for 60 seconds. The flowthrough was discarded, and additional centrifugation done, for another 5 minutes to remove residual wash buffer.

To elute the plasmid DNA, a QIAprep column was placed in a 1.5 mL microcentrifuge tube which had its cap cut off and 50 µL of water was added to the center of the filter at the bottom of the spin column, and the content was left to stand for 1 minute, after which centrifugation was finally done at 13,000 rpm for 1 minute.

The concentration of purified DNA was determined by measuring the absorbance at 260 nm and 420 nm. First the spectrophotometer was blanked with 990 µL of deionized water. A 10 µL aliquot of the plasmid DNA sample was added to a quartz cuvette containing 990 µL of water and the absorbance was taken. The concentration of DNA was calculated according to **Equation 2-5** below.

Equation 2-5: $\boldsymbol{C} = (\text{Abs}260 - \text{Abs}\ 420) \text{x}\ 50\ \text{x}\ \text{Dilution Factor}$

C) Polymerase Chain Reaction (PCR)

Table 1: A table of reactants for PCR

Mutant	gstB L114F	gstB L114F/R119A
Sterile distilled water (µL)	39	38
10x reaction buffer (µL)	5	5
Forward primer (µL)	1	1
Reverse primer (µL)	1	1
DNA template (µL)	2	3
dNTPs (µL)	1	1
DNA polymerase (µL)	1	1

Two thin-walled PCR tubes were used to assemble the reactions as shown in the Table 1. The reaction mixture was gently mixed, centrifuged briefly, and transferred to a Techne TC-312 thermocycler. The thermocycler was set to conditions presented in Table 2.

Table 2: Thermocycling conditions for PCR

Segments	PCR Cycles	Temperature	Time
1	1	95 °C	30 s
2	16	95 °C	30 s
		55 °C	1 min
		72 °C	4 min 20 s
Final extension		72 °C	2 min
Hold		4 °C	

D) Dpn I Digestion of Amplification Products

A 1 µL of the *Dpn I* restriction enzyme (10 U/ µL) was added directly to each of the amplification reactions and thoroughly mixed by gently pipetting the solution up and down. The solution was then centrifuged briefly and incubated immediately at 37 °C for 1 hour to digest parental dsDNA.

E) Transformation of XL1-Blue Super-competent Cells

Two sterile culture tubes were pre-chilled on ice before adding 50-µL of XL1-Blue super-competent cells which were thawed on ice. A 1 µL sample of *Dpn I* treated DNA from each sample reaction was transferred and mixed with separate aliquots of the super-competent cells and the content incubated on ice for 30 minutes. The cells were heat-shocked at 42 °C for 45 seconds and incubated on ice for 2 min.

After incubation, 950 µL of room temperature SOC medium was added, and the mixtures were incubated at 37 °C for 60 minutes with shaking at 225 rpm. Under sterile conditions, 200 µL of the culture was spread on plates of LB-agar containing 100 µg/mL ampicillin to select for cells that successfully took up the plasmid. The plates were incubated at 37 °C until visible colonies were observed.

F) Purification of Mutant Plasmid DNA

Four culture tubes were labelled before adding 3-mL aliquots of liquid LB containing 100 µg/mL ampicillin. The tubes were used to culture selected colonies transferred from a transformation plate. Two colonies were selected from their corresponding labelled plates and inoculated in each respective labelled tube. The cells were incubated overnight at 37

^{o}C with shaking at 200 rpm. The mutant plasmid DNA was then purified as describe above (Section 2.2.3, B)

The concentration of the mutant DNA was determined by taking the absorbance at 260 nm and 420 nm and calculated using **Equation 2-5**.

G) Transformation of E. coli BL21 (DE3) Competent Cells

E. coli BL21 (DE3) competent cells were transformed with respective purified mutant DNA plasmid as described in the Section 2.2.3 E.

H) Expression of L114F and R 119AL114F Double Mutant

Two colonies from their respective plate were isolated and inoculated in separate culture tubes each containing 5 mL of LB medium supplemented with 100 µg/mL of ampicillin. Incubation was done with shaking at 180 rpm at 37 ^{o}C until an OD_{600} of 0.6 to 1.0 was attained. IPTG was then added to a final concentration of 0.30 mM to induce protein expression. The cells were incubated overnight at 37 ^{o}C with shaking at 180 rpm.

Aliquots of the overnight bacterial culture were centrifuged at 13,000 x g for 2 minutes and the pellet obtain from each tube was analyzed for the presence of the bright protein band at 25 kDa using SDS-PAGE.

CHAPTER 3: RESULTS AND DISCUSSION

Glutathione transferases (GSTs) are important enzymes in the detoxication of xenobiotics like environmental pollutants. GstB from *E. coli* has been studied and found to be capable of catalyzing the conjugation of GSH to small electrophilic substrates like bromoacetate, converting these toxic molecules into less harmful forms.[8]

The first objective of the project was to further characterize the catalytic activities of four mutants: R119A, R119S, R119Q and R119H with respect to both bromoacetate and GSH substrates. With the aim of expanding the substrate specificity of GstB, these mutants had been created by Moore[18] via site-directed mutagenesis. The first mutant R119A (Figure 9, a) was created by replacing the positively charged amino acid residue arginine with a smaller nonpolar amino acid, alanine (A); while R119H was created by replacing the same amino acid residue, R119 with another positively charged residue, histidine (H) (Figure 9, b). Two other mutants R119S and R119Q were created by substitution of R119 residue with polar amino acids serine (S) (Figure 9, c) and glutamine (Q) (Figure 9, d), respectively.

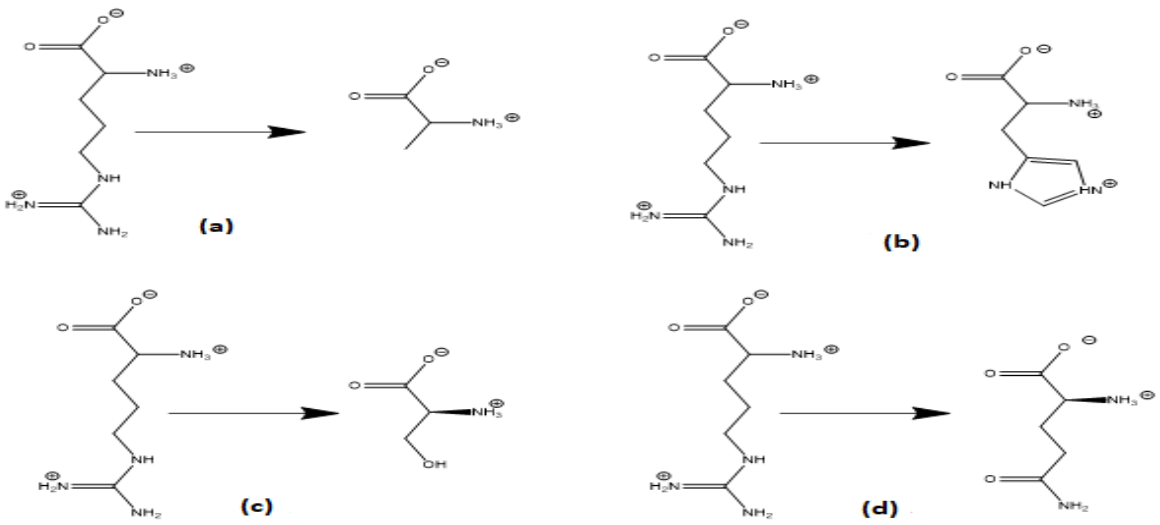

Figure 9: Structure of amino acids inserted at position 119 of the GstB polypeptide chain during site-directed mutagenesis. (a) arginine (R) replaced with alanine (A); (b) arginine (R) replaced with histidine (H); (c) arginine (R) replaced with serine (S); (d) arginine (R) replaced with glutamine (Q)

The second objective of the project was to further expand the substrate scope of GstB to accommodate electrophilic aromatic substates. Two new GstB mutants: L114F and L114F/R119A were generated. It is hoped that these mutations create an enlarged substrate binding pocket and thus able to catalyze the conjugation of GSH to aromatic electrophilic substrates like CDNB were created.

The introduction of phenylalanine (F) at the H-site of GstB was inspired by a study made by Riveron and colleagues concerning an insect *GSTe2* gene, which had a mutation in which leucine (L) at position 119 had been substituted with phenylalanine. [16] This mutation had been reported to create enough space in the substrate binding site to accommodate an electrophilic aromatic DDT molecule. Based on this study, a hypothesis was made that the introduction of phenylalanine, an aromatic hydrophobic amino acid residue, into the substrate binding site of GstB will create more room allowing for the

binding of large aromatic substrates (which are common toxicants in the environment). The L114F GstB mutant was created by substitution of leucine at position 114 of the GstB polypeptide chain with phenylalanine (Figure 10); while the second mutant, L114F/R119A was engineered using a pre-existing R119A mutant and introducing a second mutation at position 114 of the polypeptide chain, where leucine was substituted with the aromatic amino acid, phenylalanine. Since the L114F andL114F/R119A were postulated to catalyze the conjugation of GSH to electrophilic aromatic substrates, a proposal was made to characterize the two enzymes using a direct spectrophotometric assay, in which a reaction between GSH and CDNB to form GS-DNB would be monitored by measuring the absorbance at 340 nm.

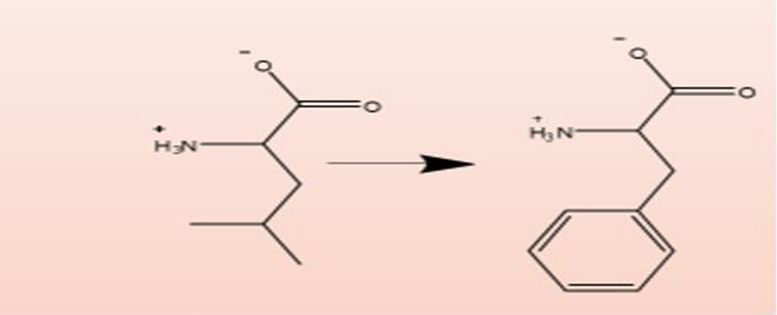

Figure 10: An image to show the aromatic structure of phenylalanine (F), an amino acid used during site-directed mutagenesis to replace leucine at position 114 of GstB, resulting in the creation of L114F.

3.1 Expression and Purification of Wild Type and Mutant Proteins R119A, R119S, R119Q, and R119H

Protein expression and purification was among the first steps in the study of wildtype (WT) and four GstB mutants: R119A, R119S, R119Q and R119H. During the expression of all five proteins, LB medium supplemented with ampicillin was used to culture transformed *E. coli* bacterial cells and the antibiotic added served to prevent the growth

of unwanted bacteria. Since *pET20b* containing the gene for GstB or mutants transformed in *E. coli*, had the gene for ampicillin resistance, selection was successfully done and only those bacteria that successfully took in the plasmid survived.

To induce protein expression, IPTG was added. Figure 11 below confirms that the sample at the beginning of purification (Lane 4) had a significant amount of GstB.

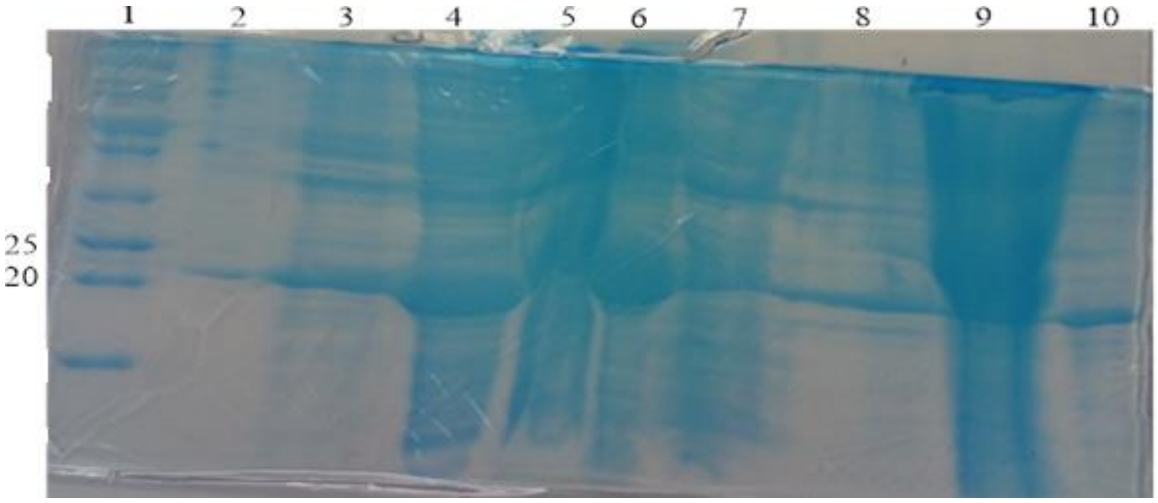

Figure 11: An image of a 12.5% SDS-PAGE gel obtained during the purification of wild type GstB. Lane 1: MW marker; Lane 2: Empty; Lane 3: Overnight bacterial culture; 4: Pre-streptomycin supernatant; Lane 5: Streptomycin pellet; 6: -Streptomycin supernatant-; Lane 7: 75% ammonium sulfate supernatant; Lane 8: Empty; Lane 9: 75% ammonium sulfate pellet; Lane 10: Empty.

During cell harvesting several rounds of centrifugation were performed, and these served in separating cells from the growth medium. Following centrifugation, the cells were subjected to 12 cycles of sonication, to break cell walls and thus release the proteins. Another round of centrifugation ensured elimination of unwanted cell debris from the lysate.

3.1.1 Ammonium Sulfate Precipitation

Ammonium sulfate precipitation was one of the techniques used to purify the wildtype and the four mutant proteins. First, the protein sample was treated with 1% streptomycin to precipitate the DNA and allow for its removal. In the next step, ammonium sulfate was added to withdraw water molecules away from the proteins, making the exposed hydrophobic groups of protein to aggregate and thus at 75% ammonium sulfate saturation, the GstB proteins were able to precipitate out of solution.

The purification step proved to be efficient in removing some of the contaminating proteins as it can be observed in Figure (12).

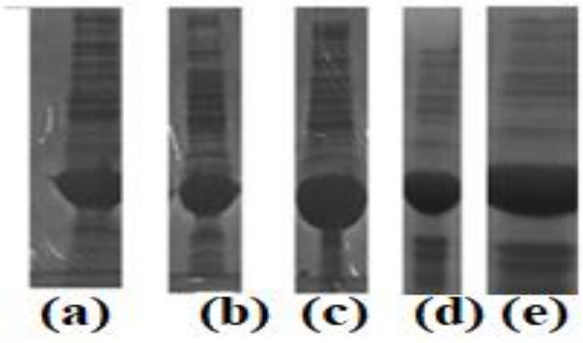

Figure 12: Images of 12.5% SDS-PAGE gel to compare the protein samples after being subjected to 75% ammonium sulfate precipitation and dialyzed overnight. (a) WT; (b) R119A; (c) R119S; (d) R119Q; (e) R119H.

3.1.2 Anion Exchange Chromatography (AEC)

Since the ammonium sulfate precipitation step alone was not sufficient to get rid of contaminating proteins, a final purification was done by anion exchange chromatography (AEC).

Q-Sepharose (Figure 14), which consisted of positively charged trimethylammonium beads was used to further purify all the five proteins. GstB having a theoretical pI of 5.05, is negatively charged at pH 7, and was able to bind to the positively charged column. Proteins that did not bind to the column were washed away using 20 mM Tris buffer, pH 7. The SDS-PAGE image in Figure 13 confirms that R119A GstB, for instance, was bound to the column as it was not observed in the wash (Lane 4), but was observed after elution (Lanes 6-11).

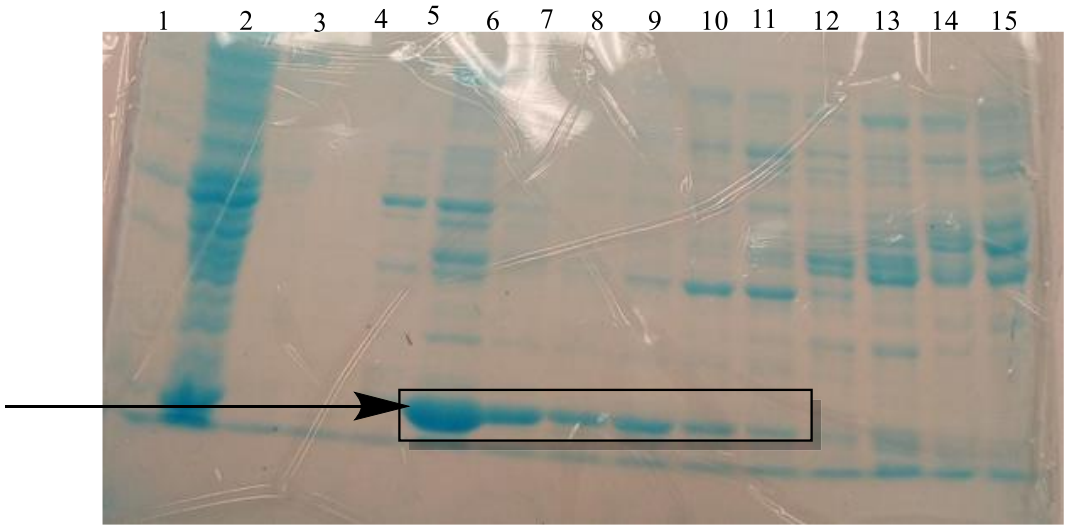

Figure 13: An image of a 12.5% SDS-PAGE gel from anion exchange chromatography column fractions collected for R119A GstB protein. Lane 1: MW marker; Lane 2: load; Lane 3: flowthrough; Lane 4: wash; Lane 5: fraction # 14; Lane 6: fraction #22; Lane 7: fraction #24; Lane 8: fraction #30; Lane 9: fraction #40; Lane 10: fraction #50; Lane 11: fraction #54; Lane 12: fraction #58; Lane 13: fraction #62; Lane 14: fraction #66; Lane 15: fraction #70

The anion exchange column proved to be effective in the purification of GstB by separating proteins based on affinity to the positively charged matrix. The proteins were eluted by a linear salt gradient. At low salt concentration weakly bound proteins were eluted, as the negatively charged chloride ions competed for charged groups on the column. Proteins with several charged groups were strongly bound to the column and

thus were eluted at higher salt concentration. Most of the GstB proteins were observed to be eluted at around 200 mM sodium chloride concentration; fractions were collected with the help of a fraction collector (Figure 14) and fractions in tubes 18 - 35 contained less contaminated GstB (Figures 13,20 to 24).

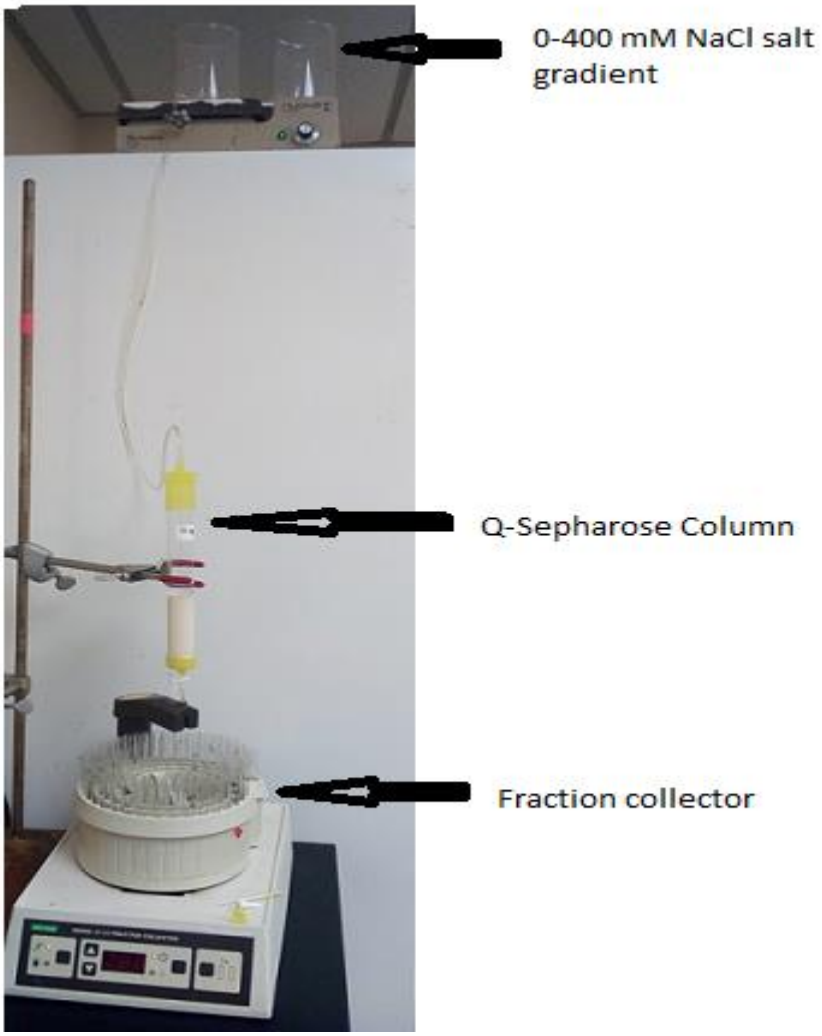

Figure 14: An image of a Q-Sepharose anion exchange chromatography setup used in the purification of GstB proteins. The proteins bound to the column were eluted using a 0-400 mM NaCl salt gradient and the fraction collector was set to collect fractions at 3 minutes intervals.

Following AEC, collected fractions were tested for presence and amount of protein by measuring absorbance at 280 nm using a spectrophotometer. The data obtained from the

analysis was plotted in graphs. Figures 15 - 19 show the relationship between the absorbance at 280 nm and fractions collected during AEC for WT, R119A, R119S, R119Q, and R119H.

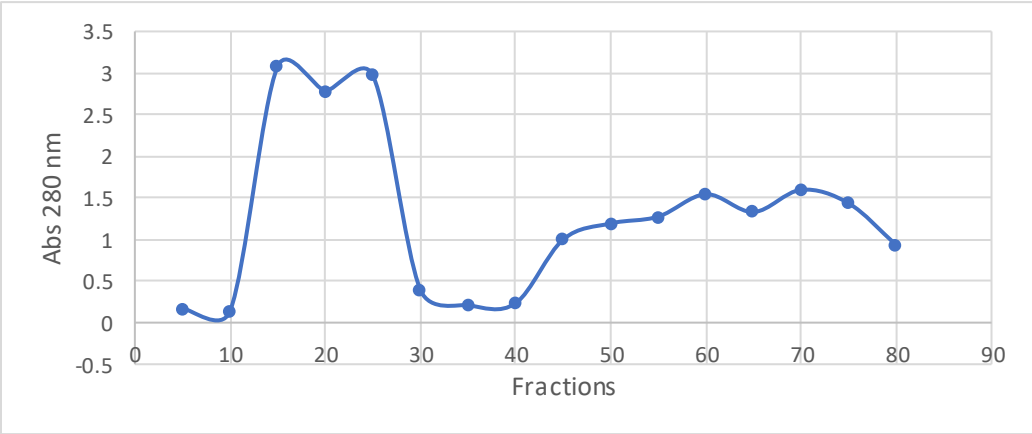

Figure 15: A plot of absorbance at 280 nm versus anion exchange fractions of wild type protein eluted with a 0-400 mM sodium chloride salt gradient prepared in 20 mM NaP_i, pH 7. Fractions were collected using a fraction collector.

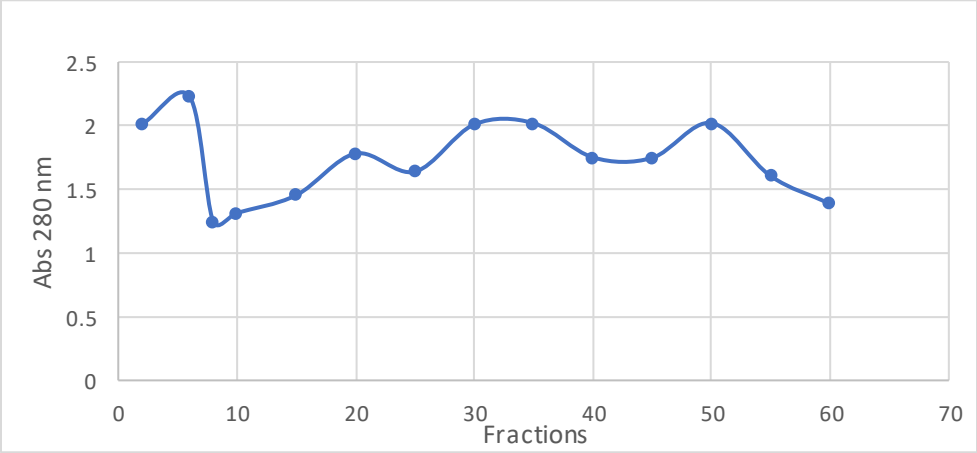

Figure 16: A plot of absorbance at 280 nm versus anion exchange fractions of R119A GstB mutant eluted with a 0-400 mM sodium chloride salt gradient prepared in 20 mM NaP_i, pH 7. Fractions were collected using a fraction collector.

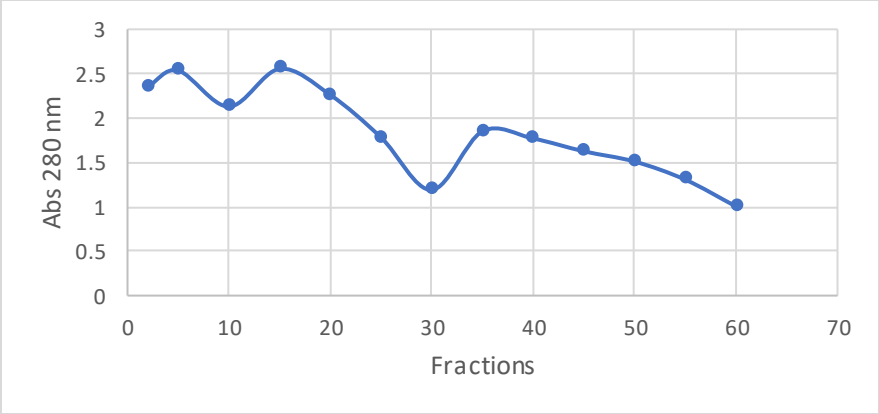

Figure 17: A plot of absorbance at 280 nm versus anion exchange fractions of R119S GstB mutant eluted with a 0-400 mM sodium chloride salt gradient prepared in 20 mM NaP_i, pH 7. Fractions were collected using a fraction collector.

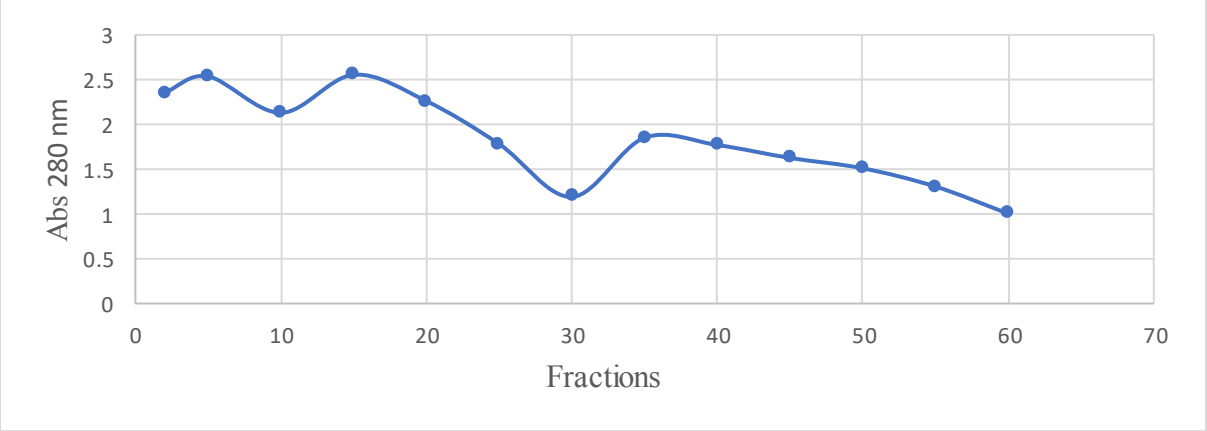

Figure 18: A plot of absorbance at 280 nm versus anion exchange fractions of R119Q GstB mutant eluted with a 0-400 mM sodium chloride salt gradient prepared in 20 mM NaP_i, pH 7. Fractions were collected using a fraction collector.

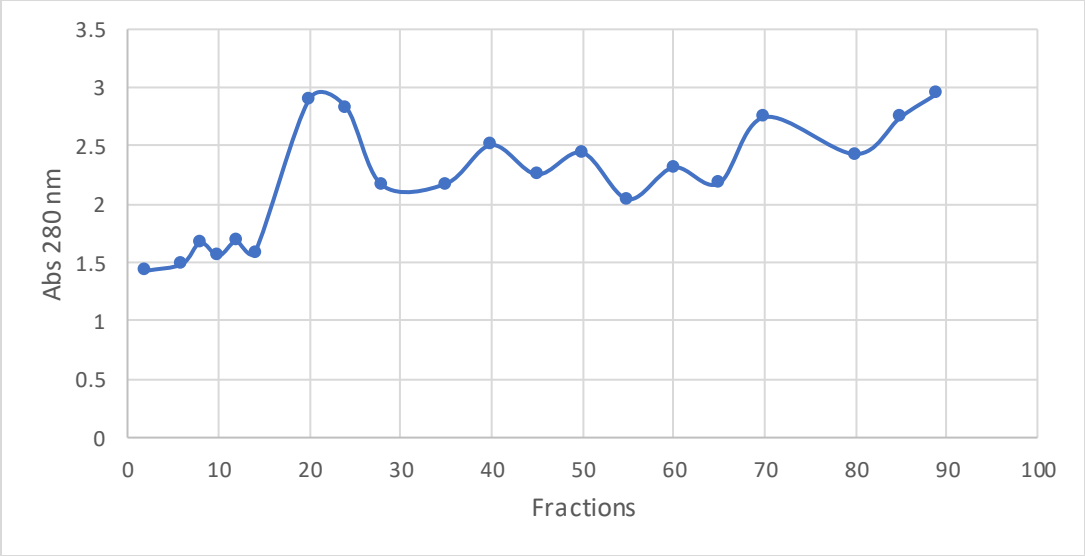

Figure 19:A plot of absorbance at 280 nm versus anion exchange fractions of R119H GstB mutant eluted with a 0-400 mM sodium chloride salt gradient prepared in 20 mM NaP_i, pH 7. Fractions were collected using a fraction collector.

3.1.3 Validation of the Presence of GstB Protein in Fractions

An SDS-PAGE was used to test the fractions for presence of GstB protein. The electrophoresis method was able to separate the proteins' individual subunits based on their molecular weight; where high molecular weight polypeptides traveled less on gel while small molecular weight proteins traveled further down the gel with the application of current. The pore sizes on the matrix were determined by the concentration of polyacrylamide and thus 12.5% SDS-PAGE gels were prepared and used for all analysis. From the SDS-PAGE gels, it was easy to not only identify the fractions that had GstB protein, but also the quality of the harvested fractions. Identification of GstB protein was based on its position on the gel. Standard molecular weight markers were run along with the protein samples and this allowed for identification of the proteins on the gels. The bands representing GstB protein were observed at around 25 kDa, which was in line with the stated molecular weight of an individual GstB subunit from literature.[28]

The purity of GstB in the fractions was determined on the gels based on the number of contaminating bands on the lanes bearing the 25 kDa bands. Fractions that showed a GstB band and fewer of the contaminating bands were taken to be significantly pure. The results of SDS-PAGE analyses for all proteins are shown in Figures 20 to 24.

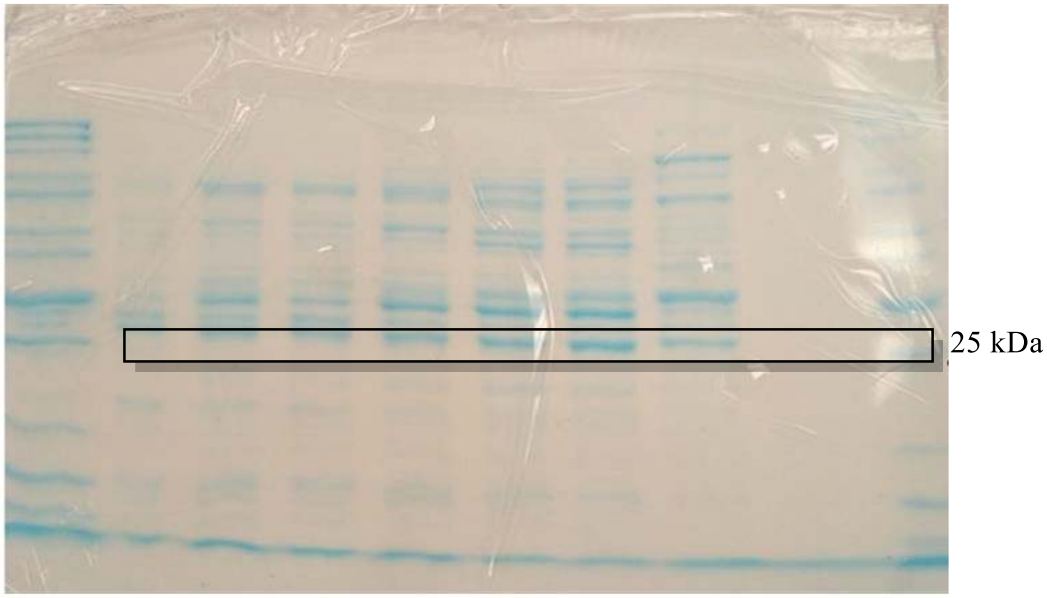

Figure 20: An image of a 12.5% SDS-PAGE gel of anion exchange chromatography column fractions collected during the purification of wild type GstB. Lane 1: fraction #5; Lane 2: fraction # 18; Lane 3: fraction #28; Lane 4: fraction #32 Lane 5: fraction # 35; Lane 6: fraction #40; Lane 7: fraction #45; Lane 8: fraction #50; Lane 9: empty; Lane 10: MW marker.

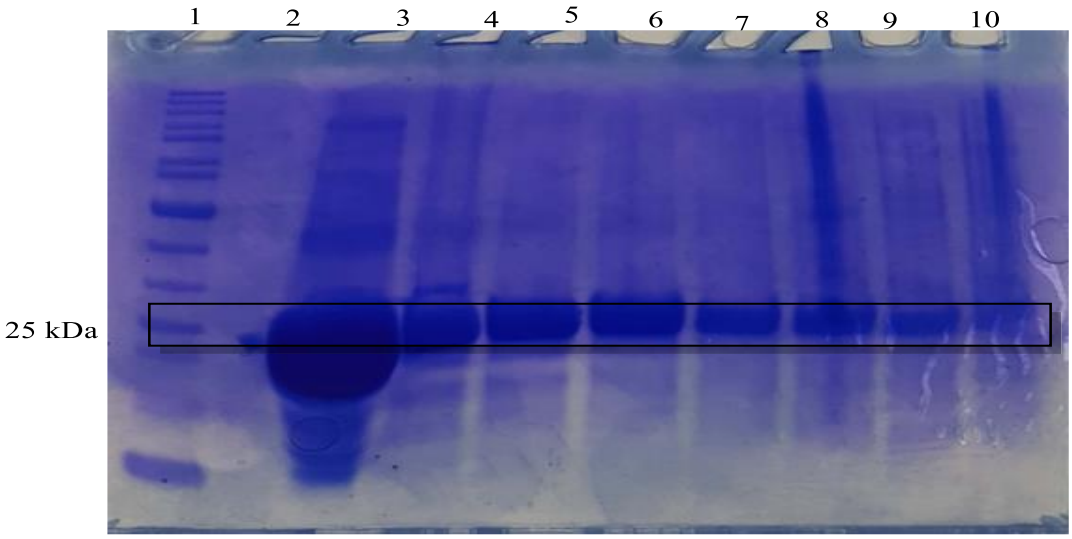

Figure 21: An image of a 12.5% SDS-PAGE gel of anion exchange chromatography column fractions collected during the purification of R119S GstB protein. Lane 1: MW marker; Lane 2: flowthrough; Lane 3: load; Lane 4: fraction # 15; Lane 5: fraction # 20; Lane 6: fraction #25; Lane 7: fraction #32; Lane 8: fraction #38; Lane 9: fraction #43; Lane 10: fraction #48.

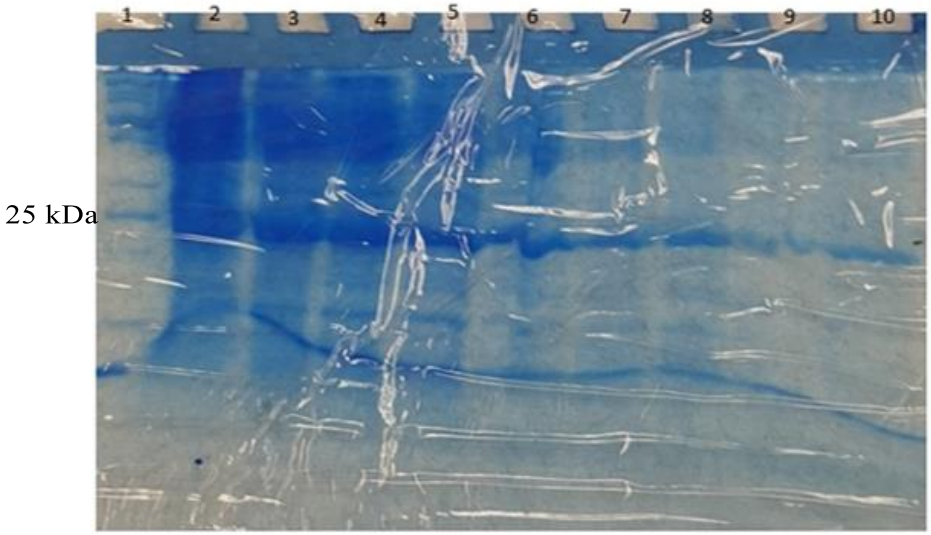

Figure 22:An image of a 12.5% SDS-PAGE gel of anion exchange chromatography column fractions collected during the purification of R119Q GstB protein. Lane 1: MW marker; Lane 2: load; Lane 3: fraction #10; Lane 4: fraction # 15; Lane 5: fraction # 18; Lane 6: fraction #25; Lane 7: fraction #29; Lane 8: fraction #35; Lane 9: fraction #38; Lane 10: fraction #42.

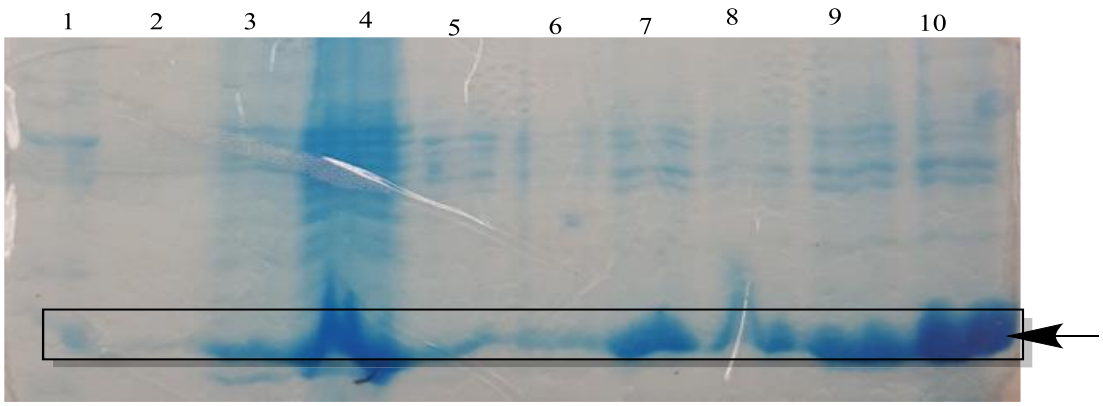

Figure 23:An image of a 12.5% SDS-PAGE gel of anion exchange chromatography column fractions collected during the purification of R119H GstB protein. Lane 1: MW marker; Lane 2: wash; Lane 3: flowthrough; Lane 4: load; Lane 5: fraction # 20; Lane 6: fraction #25; Lane 7: fraction #30; Lane 8: fraction #35; Lane 9: fraction #40; Lane 10: fraction #45.

After the fractions containing GstB (or a mutant) were combined and concentrated, a final SDS-PAGE was done to validate the purity of the proteins before they were used in any assays. An SDS PAGE for all the five proteins (Figure 25), confirms that the concentrated protein samples had satisfactory purity for kinetic studies. Figure 24 (Lane 5) shows that the final combined fractions from the purification of R119A mutant, was significantly pure.

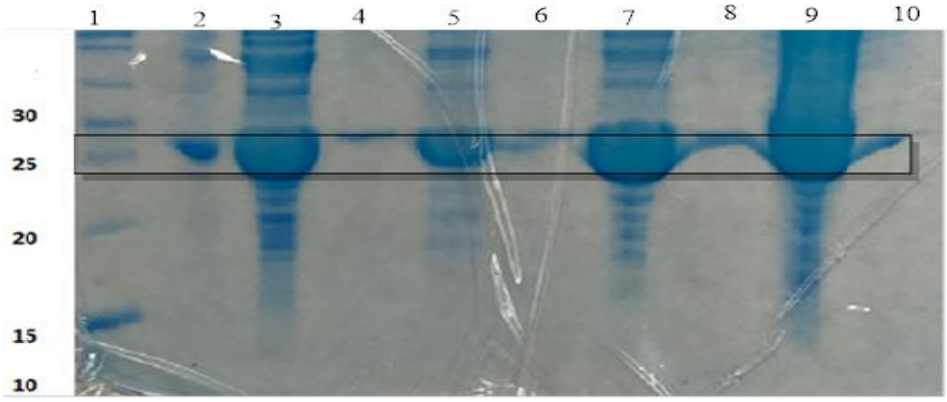

Figure 24: An image of a 12.5% SDS-PAGE gel of concentrated fractions of R119A GstB protein. Lane 1: MW marker; Lane 2: empty; Lane 3: fractions #49-#54; Lane 4: empty;

Lane 5: fraction # 25- #38; Lane 6: empty; Lane 7: fraction #39- #45; Lane 8: empty; Lane 9: fraction #18- #21; Lane 10: empty

.

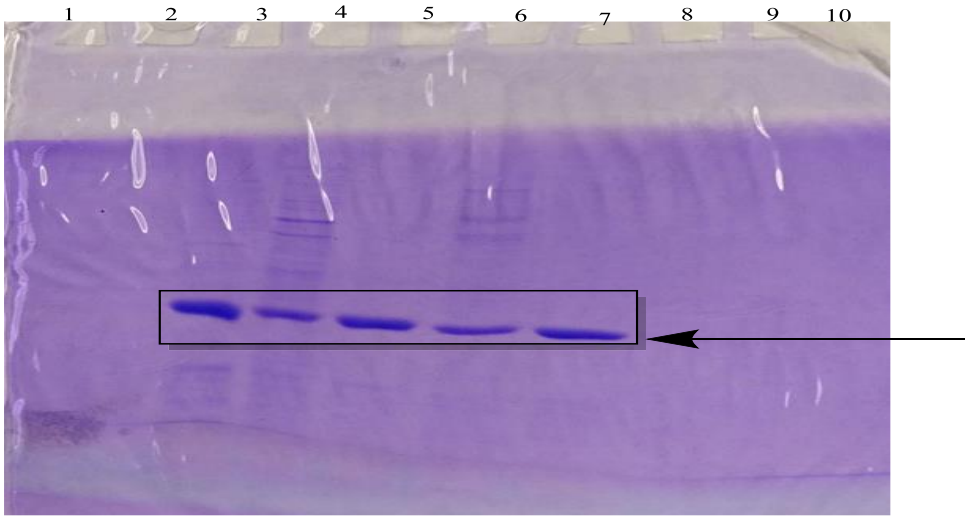

Figure 25: An image of a 12.5% SDS-PAGE gel of combined fractions of wildtype and mutant proteins. Lane 1: empty; Lane 2: empty; Lane 3: wildtype 20-fold diluted combined fractions #15-#25; Lane 4: R119H; Lane 5: R119A; Lane 6: R119Q; Lane 7: R119S; Lanes 8 - 10: empty.

3.1.4 Creation and Expression of L119F and R119A.L114F Mutants

Using site-directed mutagenesis, two mutants L114F andL114F/R119A were created.

The first step was to design the primers bearing the desired mutation for each mutant. For L114F, the forward and reverse primers each consisted of 37 nucleotides, with an introduced mutation in which the CTG codon for leucine (L) was replaced with a TTT codon for phenylalanine (F), as shown below.

Forward primer L114F: 5'gctcatcgcgggatc**ttt**atgggattagtcagaacac-3'

Reverse primer L114F: 5'-gtgttctgactaatcccat**aaa**gatcccgcgatgagc-3'

The L114F/R119A primers also had 37 nucleotides with two inserted mutations. The first mutation involved a substitution of a CTG codon for L with a codon TTT for F; while the second mutation, involved a substitution of AGA codon for arginine (R), with a GCA codon for alanine (A), as shown below.

Forward primer L114F, R119A: 5'-gctcatcgcgggatc**ttt**atgggattagtc**gca**acac-3'

Reverse primer L114F, R119A: 5'- gtgt**tgc**gactaatcccat**aaa**gatcccgcgatgagc-3'

It was important to design primers with the melting temperature (T_m) that was suitably low to permit the primers to anneal to the DNA template during PCR, but also not too low as to allow the formation of nonspecific duplexes. Tm of the primers was calculated to be 78.5 ^oC for the L114F and 79.5 ^oC for theL114F/R119A double mutant.

For the L114F GstB mutant, the T_m was calculated as shown below.

T_m= 81.5 + 0.41 (%GC) - (675/N) – (% Mismatch)

N=37; GC = 18; (18/37) x 100% = 49%; % mismatch = (2/37) x100% = 5%

Tm= 78.5 ^oC

For the L114F/R119A GstB mutant, the T_m was calculated as shown below.

N=37; GC = 19; (19/37) x 100% = 51%; % mismatch = (2/37) x100% = 5%

T_m= 79.5 ^oC

After the primers had been designed and synthesized, DNA templates were purified using QIAprep Spin Miniprep Kit. The absorbance of the purified DNA was taken at 260 nm and the concentration was calculated to be 29 µg/mL and 13 µg/mL for *pET20b-gstB* and

pET20b-gstB R119A template, respectively. The amount was thus confirmed to be enough for use in the next step. Polymerase chain reaction enabled adequate amplification of the plasmid DNA for successful transformation. The use of high-fidelity DNA polymerase reduced the chances of introducing unwanted mutations. The PCR thermocycling conditions were set for efficient amplification. To separate the double stranded DNA template into single strands, the denaturation temperature was set at 95 °C. The annealing temperature was set at 55°C to allow specific binding of the primers to the complementary DNA strand, while the extension temperature was increased to 72 °C for effective incorporation of dNTPs by the DNA polymerase. Following PCR, the amplification products were treated with *Dpn I* restriction enzyme to select for mutated plasmids. The enzyme was able to digest methylated parental DNA leaving the newly synthesized DNA containing the desired mutation. The amplified product was transformed into XL1-Blue super-competent cells to achieve colonies containing the needed plasmids. The plasmid DNA was finally harvested from XL1-Blue super-competent cells and purified using QIAprep Spin Miniprep Kit, before being transformed into BL21 (DE3) competent cells.

The transformed *E. coli* BL21 (DE3) cells were first grown on LB - agar selection plates and later inoculated in LB medium supplemented with ampicillin. Protein expression was induced by addition of IPTG. After IPTG induction, the overnight bacterial culture was centrifuged at 13,000 x g for 3 minutes and the pellet was analyzed to check if the cells were able to express the desired protein. SDS-PAGE was performed to look for the presence of a 25 kDa band, representing a GstB protein. Figure 26 shows several bands on lanes 2 and 3. Among these protein bands observed, is a prominent band of

approximately 25 kDa located in each lane; the bands corresponds to the two GstB mutants' proteins.

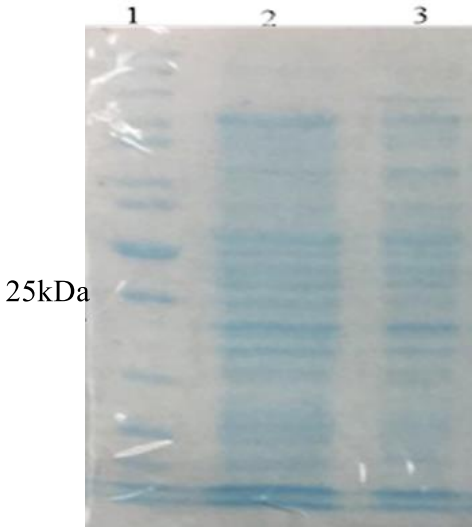

Figure 26:An image of a 12.5% SDS-PAGE gel done on bacterial culture containing pET20 -gstB L114F and L114F/R119A after IPTG induction. Lane 1: MW marker; Lane 2: L114F/R119A overnight; Lane 3: L114F overnight.

3.2 Activity Testing of Wild Type and Mutant Proteins

To determine the effects of the mutation of arginine 119 on the catalytic properties of GstB enzymes, kinetic assays were done using bromoacetate (electrophile) and GSH as substrates. During the reactions, the concentration of one substrate was kept at a constant, non-limiting concentration while the concentration of the second substrate was varied. The bromoacetate-GSH conjugation reaction was monitored using a discontinuous spectrophotometric assay. In this assay, the reaction aliquot was transferred to a cuvette where the GSH reacted with 5,5'-dithio-bis-(2- nitrobenzoic acid) (DTNB) at pH 8. The reaction yields a mixed disulfide product and 2-nitro-5-thiobenzoate dianion (TNB^{2-}) which absorbs light at 412 nm.

Aliquots of the reaction mixture were taken before and after a two-minute incubation, transferred into a cuvette containing DTNB, and the absorbance was measured at 412 nm. The assay allowed for determination of the amount of GSH remaining at the end of each spontaneous and catalyzed reaction. The initial and final concentrations of GSH for each of these reactions were calculated and used to determine the rate of reaction. Since GSH is known to react spontaneously with an electrophile, the rates of both the spontaneous and catalyzed reaction were monitored. By subtracting the rate of the spontaneous (uncatalyzed) reaction from the rate of catalyzed reaction, the adjusted rate of reaction was determined.

The values of Michaelis constant (K_M), maximal velocity (V_{max}), and inhibition constant (K_i) were obtained by fitting the acquired rate data into the Michaelis-Menten equation accounting for substrate inhibition (**Equation 2-3**)

3.2.1 GstB Enzyme Activity Assay with Varying Bromoacetate Concentration

Wild type GstB (WT) and four-mutants: R119A, R119S, R119Q and R119H were screened for activity and the data was analyzed. The rate of bromoacetate conjugation with GSH catalyzed by the GstB enzymes was fitted into a Michaelis-Menten model accounting for substrate inhibition since the substrate, bromoacetate was observed to inhibit the reaction at high concentration. The results are presented in graphs (Figures 27 to 31).

The Michaelis constant, K_M, of the enzymes for bromoacetate indicated that the WT, R119A, R119S and R119H were able to bind to the bromoacetate substrate with equal affinity. The three enzymes all had a K_M of 6 mM (Figures 27 to 29 and 31). The R119Q

mutant, on the other hand, had a lower affinity for bromoacetate with a K_M of 8 mM (Figure 30).

Comparison of data from the modelled graphs suggested that the R119A mutant (Figure 28) experienced the highest inhibitory effect from the bromoacetate substrate, recording the lowest K_i of 10 mM. The other four enzymes were also inhibited by bromoacetate, with WT and R119Q mutants recording a K_i of 25 mM (Figure 27 and 30). The R119S and R119H mutants experienced a lower inhibitory effect from the substrate, having almost the same K_i of 27 mM and 28 mM, respectively (Figure 29 and 31).

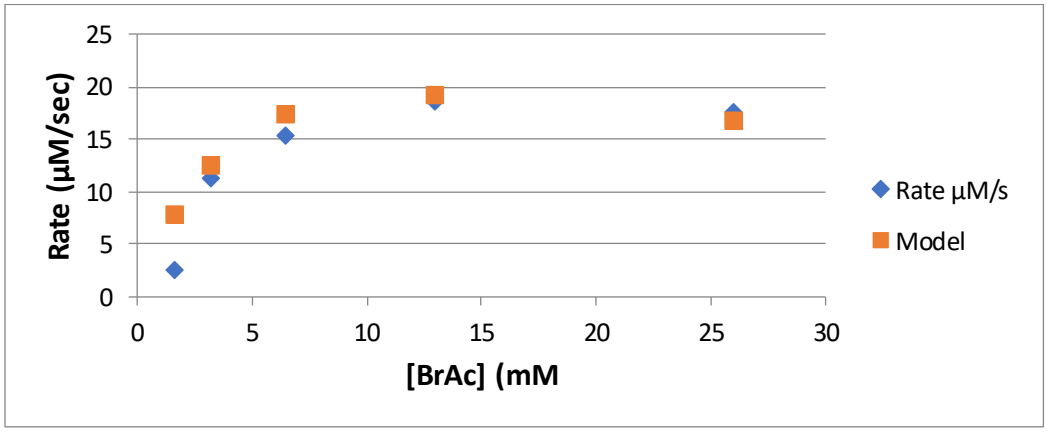

Figure 27: A plot of the rate of bromoacetate-GSH conjugation catalyzed by wildtype GstB versus bromoacetate concentration with experimental rate (blue) and model rate (orange); $K_{M=}$ 6 mM; V_{max}=38 µM/sec; K_i= 25 mM; [BrAc]= 1.6-26 mM; [GSH]=5 mM; [GstB]= 1.4 µM; R^2: 0.97; Reaction time: 2 min.

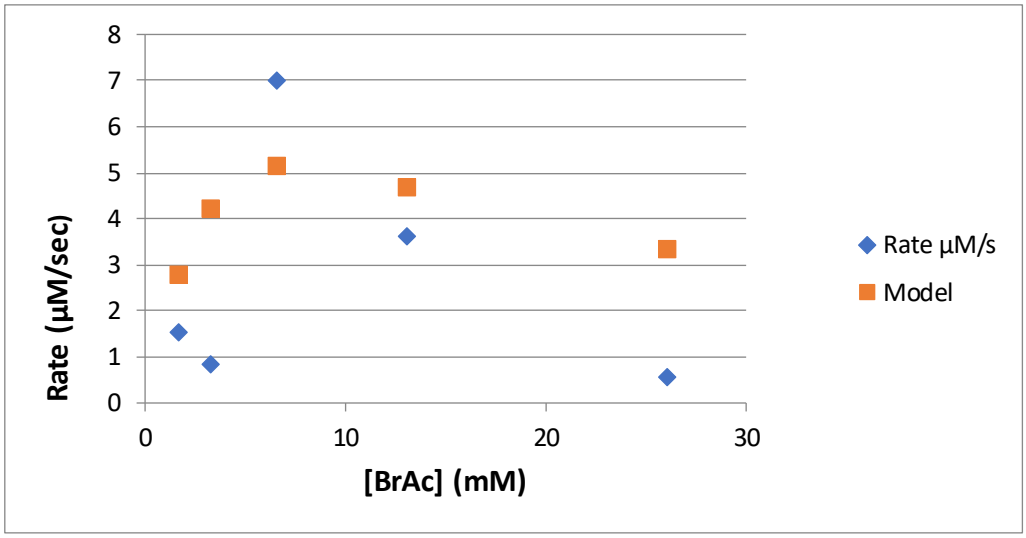

Figure 28: A plot of the rate of bromoacetate-GSH conjugation catalyzed by R119A GstB versus bromoacetate concentration with experimental rate (blue) and model rate (orange); K_M= 6 mM; V_{max}=13 µM/sec; K_i= 10 mM; [BrAc]= 1.6-26 mM; [GSH]= 5 mM; [GstB R119A]= 1.4 µM; R^2: 0.77; Reaction time: 2 min.

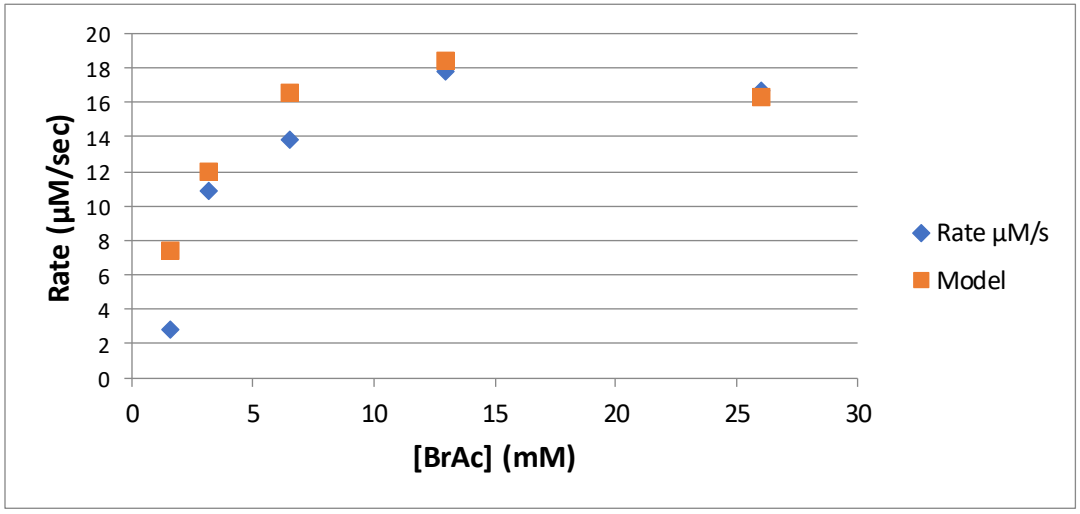

Figure 29: A plot of the rate of bromoacetate-GSH conjugation catalyzed by R119S GstB versus bromoacetate concentration with experimental rate (blue) and model rate (orange); K_M= 27 mM; V_{max}=36 µM/sec; K_i= 27 mM; [BrAc]= 1.6-26 mM; [GSH]=5 mM; [GstB R119S] = 1.4 µM; R^2: 0.97; Reaction time: 2 min.

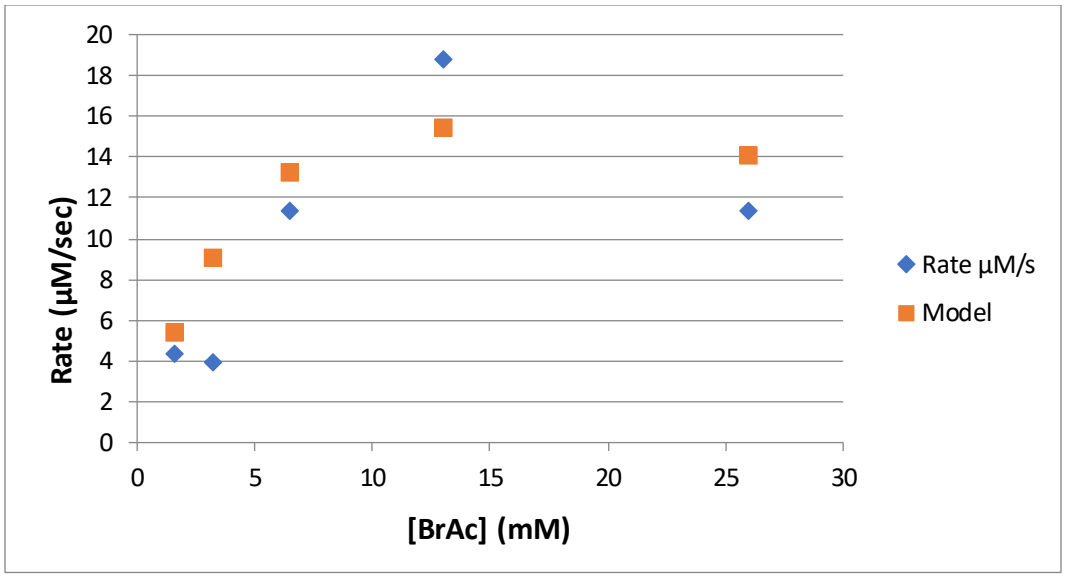

Figure 30: A plot of the rate of bromoacetate-GSH conjugation catalyzed by R119Q GstB versus bromoacetate concentration with experimental rate (blue) and model rate (orange); K_M= 8 mM; V_{max}=33 µM/sec; K_i = 25 mM; [BrAc]= 1.6-26 mM; [GSH]=5 mM; [GstB R119Q] = 1.4 µM; R^2: 0.94; Reaction time: 2 min

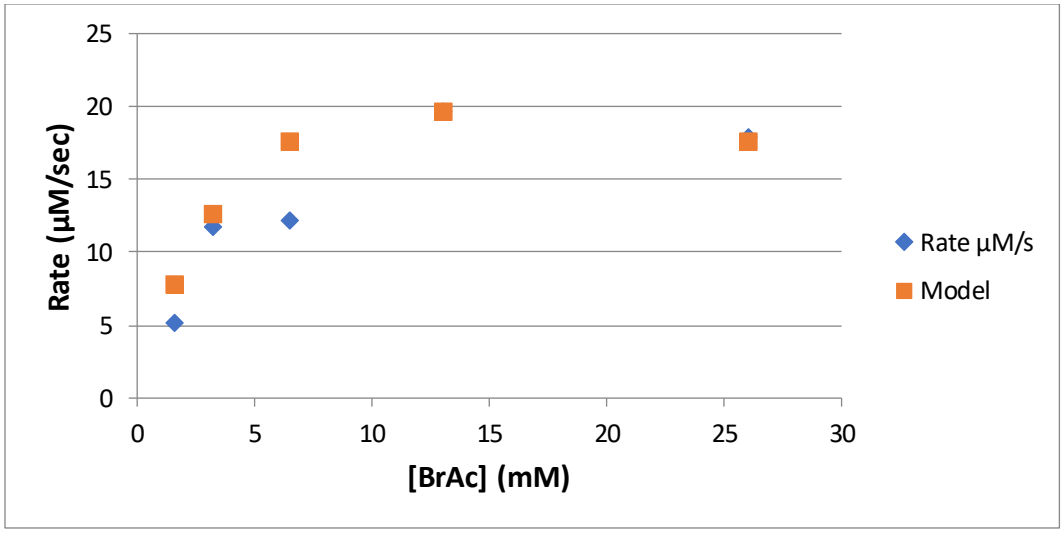

Figure 31: A plot of the rate of bromoacetate-GSH conjugation catalyzed by R119H GstB versus bromoacetate concentration with experimental rate (blue) and model rate (orange); K_M= 6 mM; V_{max}=38 µM/sec; K_i= 28 mM; [BrAc]= 1.6-26 mM; [GSH]=5 mM; [GstB R119H] = 1.4 µM; R^2: 0.97; Reaction time: 2 min.

3.2.2 GstB Enzyme Activity Assay with Varying Glutathione Concentration

While varying GSH concentration and keeping the concentration of bromoacetate constant at 18 mM; the rate of bromoacetate conjugation with GSH catalyzed by the GstB enzymes was determined and modeled with inhibition because GSH was observed to inhibit the reaction at high concentration, just like bromoacetate (Figures 32 to 36).

Values for the Michaelis constant were analyzed and the data indicated that wild type GstB and the R119Q mutants had the highest affinities for GSH, as both recorded a K_M of 5 mM (Figures 32 and 35). The R119H mutant followed closely with a K_M of 7 mM (Figure 36), while R119A had the lowest affinity of all the five enzymes, with a K_M of 15 mM (Figure 33).

The inhibitory effects of GSH in the reaction was also studied (Figure 39) and the data suggested that the R119H mutant (Figure 36) experienced the highest inhibitory effect from GSH substrate, recording the lowest K_i of 13 mM, as compared the other enzymes. R119A mutant, also followed closely, with the second lowest recorded K_i value of 17 mM (Figure 33). The wild type and R119Q mutant had nearly the same K_i of 23 mM and 24 mM, respectively (Figure 32 and 35). The intensity of inhibition experienced by the R119S mutant from GSH was found to be very weak as indicated by the recorded highest K_i of 53 mM (Figure 34).

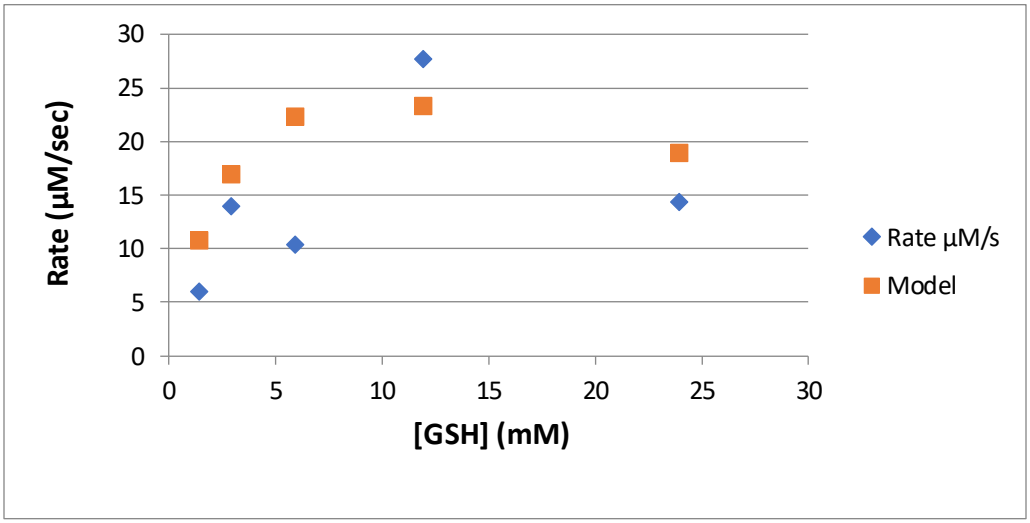

Figure 32: A plot of the rate of bromoacetate-GSH conjugation catalyzed by wildtype GstB versus GSH concentration with experimental rate (blue) and model rate (orange); K_M =5 mM; V_{max}=50 µM/sec; $K_{i,}$ = 17 mM; [GSH]= 1.5-24 mM; [BrAc]= 18 mM; [GstB]= 1.4 µM; R^2: 0.89; Reaction time: 2 min

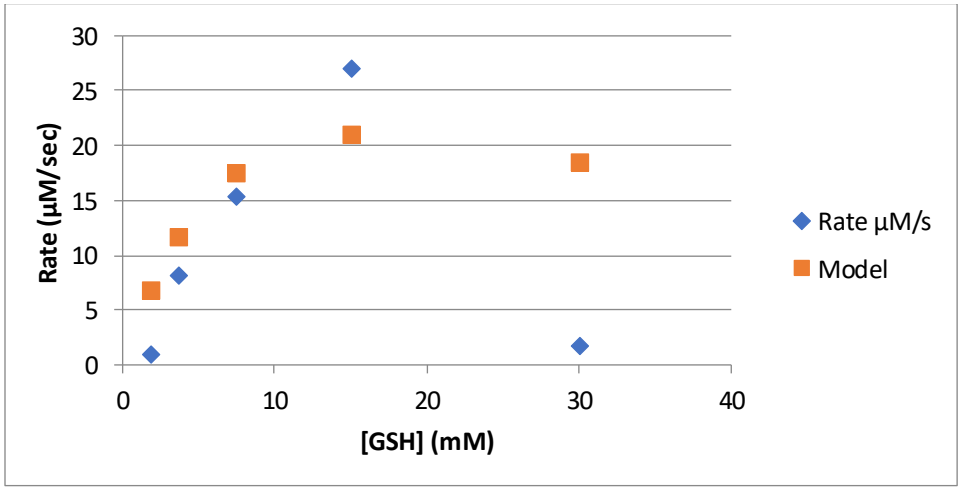

Figure 33: A plot of the rate of bromoacetate-GSH conjugation catalyzed by R119A GstB versus GSH concentration with experimental rate (blue) and model rate (orange); K_M=15 mM; V_{max}=60 µM/sec; K_i = 17 mM; [GSH]= 1.9-30 mM; [BrAc]=18 mM; [GstB R119A] = 1.4 µM; R^2: 0.77; Reaction time: 2 min

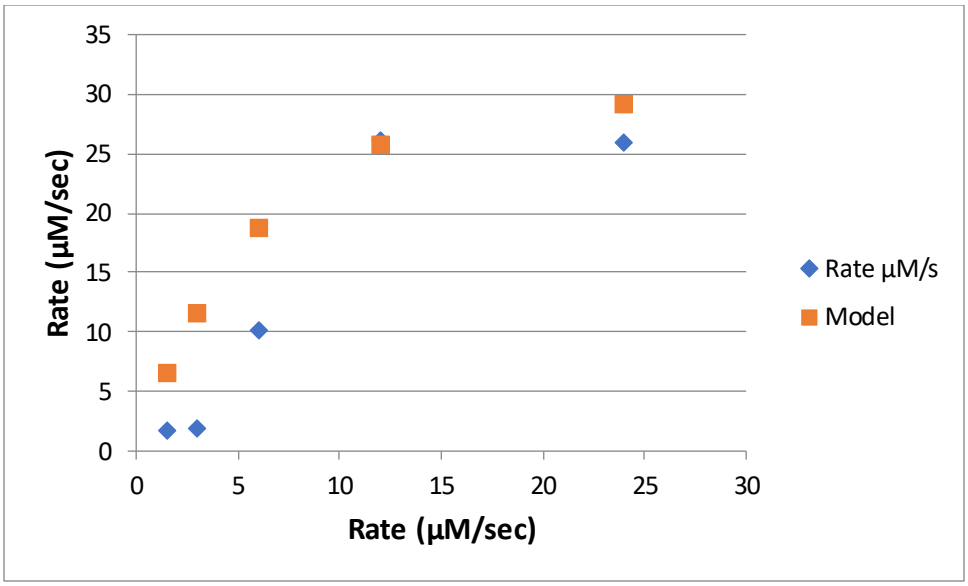

Figure 34: A plot of the rate of bromoacetate-GSH conjugation catalyzed by R119S GstB versus GSH concentration with experimental rate (blue) and model rate (orange); K_M =11 mM; V_{max}=55 µM/sec; K_i = 53 mM; [GSH]= 1.5-24 mM; [BrAc]=18 mM; [GstB R119S] = 1.4 µM; R^2: 0.90; Reaction time: 2 min

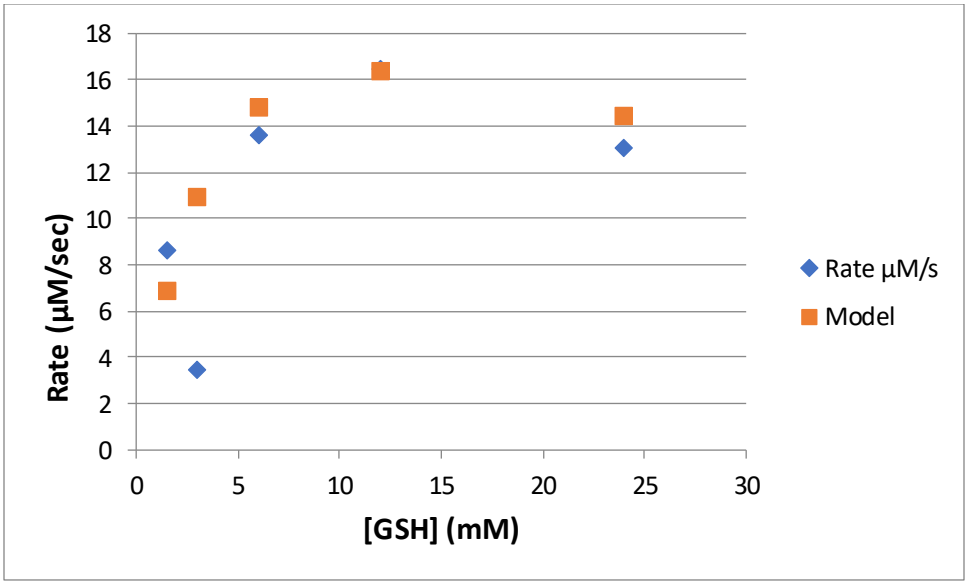

Figure 35: A plot of the rate of bromoacetate-GSH conjugation catalyzed by R119Q GstB versus GSH concentration with experimental rate (blue) and model rate (orange); K_M =5 mM; V_{max}=32 µM/sec; K_i= 24 mM; [GSH]= 1.5-24 mM; [BrAc]=18 mM; [GstB R119Q] = 1.4 µM; R^2: 0.94; Reaction time: 2 min

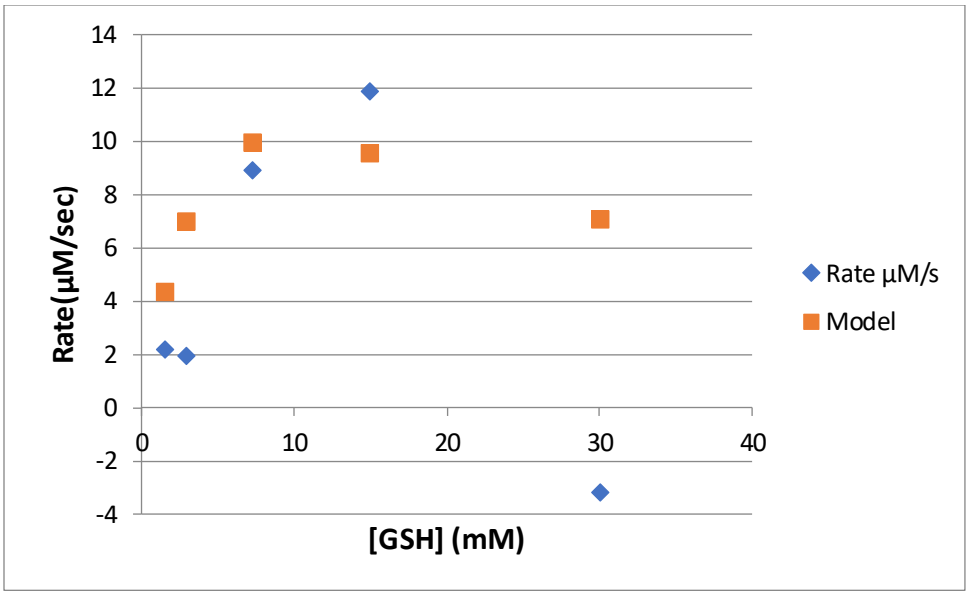

Figure 36:A plot of the rate of bromoacetate-GSH conjugation catalyzed by R119H GstB versus GSH concentration with experimental rate (blue) and model rate (orange); K_M=7 mM; V_{max}=25 µM/sec; K_i = 17 mM; [GSH]= 1.5-30 mM; [BrAc]=18 mM; [GstB R119H] = 1.4 µM; R^2: 0.68; Reaction time: 2 min

3.2.3 Kinetic Parameters

The activity of the five enzymes were studied in relation to both bromoacetate and GSH and the kinetic parameters are summarized in a table (Table 3) and illustrated using bar graphs (Figures 37 to 39). The turnover number (k_{cat}), which is a catalytic constant that indicates how fast a substrate is converted to product, was recorded for all the enzymes. With respect to bromoacetate, the study found the R119H mutant and wildtype had the highest k_{cat} of 27 sec^{-1} followed closely by wildtype with a k_{cat} of 25 sec^{-1}. Both R119Q and R119S had a k_{cat} of 24 sec^{-1} .The R119A mutant had the lowest k_{cat} of 9 sec^{-1}. Keeping the concentration of bromoacetate constant and varying the concentration of GSH, R119A was able to outperform all the other enzymes with a k_{cat} of 43 sec^{-1} followed closely by R119S which had a k_{cat} of 39 sec^{-1}. The R119H had the lowest k_{cat} of 18 sec^{-1}.

The relationship between k_{cat} and K_M (k_{cat}/K_M), which is a ratio that is used to gauge the catalytic efficiency of an enzyme, was calculated for the wildtype and mutant enzymes and results were plotted in a bar graph (Figure 39). With the concentration of GSH kept constant while varying the concentration of bromoacetate, the R119S, R119H and wildtype recorded approximately the same k_{cat}/K_M of 6 mM^{-1}, sec^{-1} 5 mM^{-1} sec^{-1} and 4 mM^{-1} sec^{-1} respectively. The R119A, had the lowest values of k_{cat}/K_M of 2 mM^{-1} sec^{-1} (Table 3).

With the concentration of bromoacetate kept constant while varying the concentration of GSH, the wildtype had the highest ratio of k_{cat}/K_M of 7 mM^{-1} sec^{-1}, followed closely by R119Q with a k_{cat}/K_M of 5 mM^{-1} sec^{-1}. The mutant R119A and R119H, had the lowest catalytic efficiency of 3 mM^{-1} sec^{-1}.

Table 3: A table of kinetic parameters with varying concentration of both GSH and bromoacetate substrates, respectively.

	Varying [GSH]					Varying [BrAc]				
Kinetic parameter	WT GstB	R119A	R119S	R119Q	R119H	WT GstB	R119A	R119S	R119Q	R119H
K_M (mM)	5 ± 0.2	15± 0.2	11± 0.1	5± 0.1	7± 0.2	6± 0.1	6± 0.1	6± 0.2	8± 0.2	6± 0.2
k_{cat} (sec^{-1})	36± 0.2	43± 0.2	39± 0.1	23± 0.1	18± 0.2	25± 0.1	9± 0.1	24± 0.2	24± 0.2	27± 0.2
k_{cat}/K_M (mM^{-1} sec^{-1})	7± 0.2	3± 0.2	4± 0.1	5± 0.1	3± 0.2	4 ± 0.1	2± 0.1	6± 0.2	3± 0.2	5 ± 0.2
Ki (mM)	17± 0.2	17± 0.2	53± 0.1	24± 0.1	13± 0.2	25± 0.1	10± 0.1	27± 0.2	25± 0.2	28± 0.2

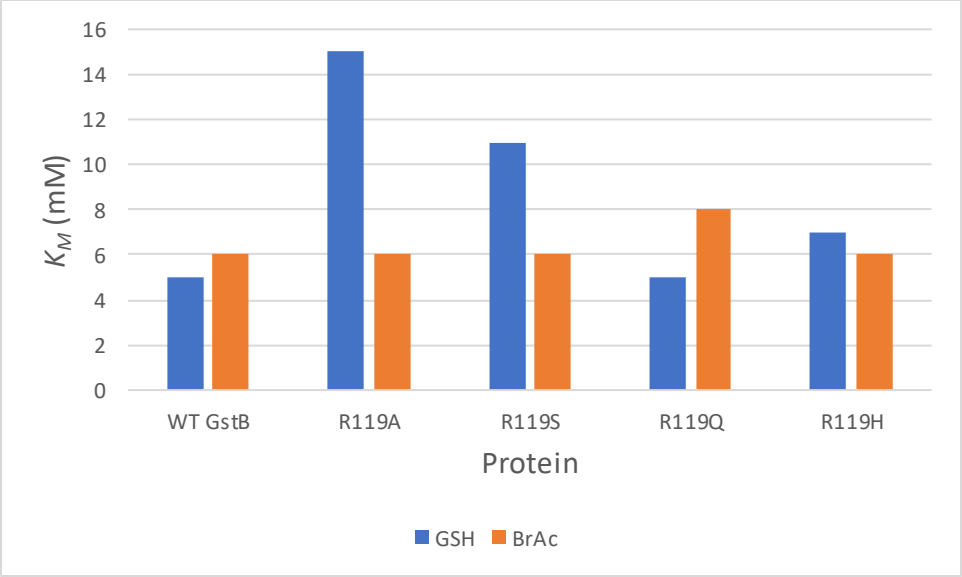

Figure 37: A bar graph to compare the K_M of wild type and mutant proteins: R119H, R119S, R119Q and R119A; with respect to both GSH (blue) and bromoacetate (orange) substrates.

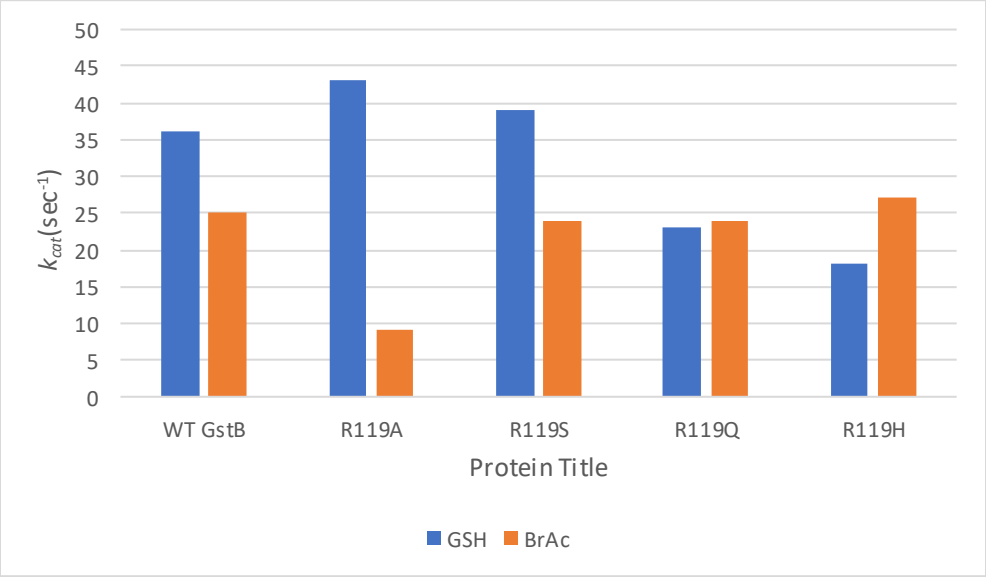

Figure 38: A bar graph to compare the k_{cat} of wild type and mutant proteins: R119H, R119S, R119Q and R119A; with respect to both GSH (blue) and bromoacetate (orange) substrates.

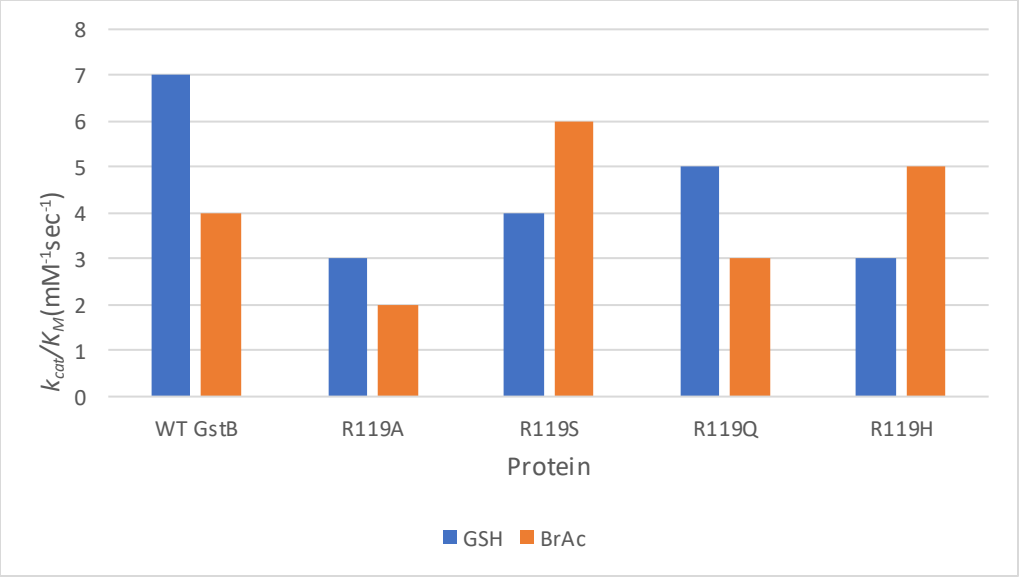

Figure 39: A bar graph to compare the k_{cat}/K_M of wild type and mutant proteins: R119H, R119S, R119Q and R119A; with respect to both GSH (blue) and bromoacetate (orange) substrates.

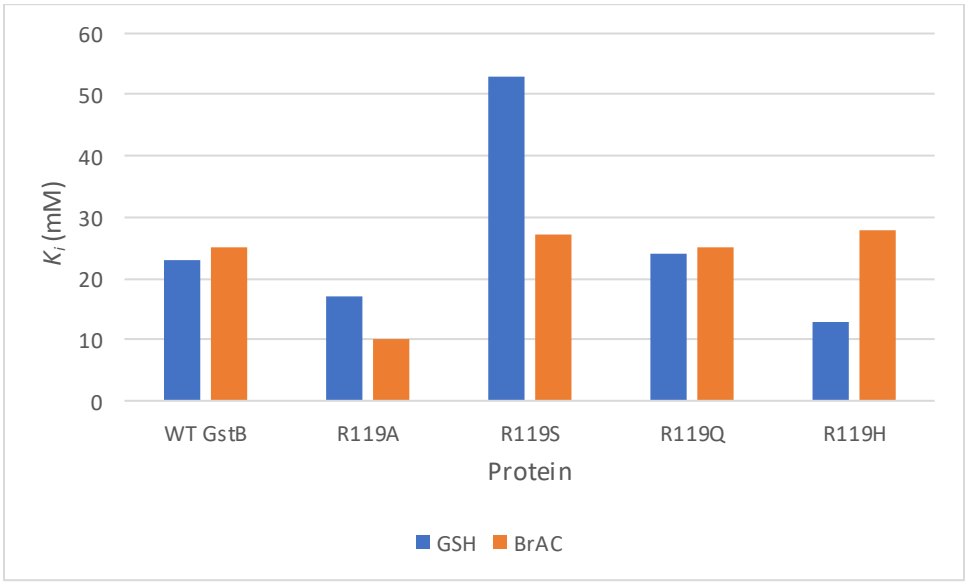

Figure 40: A bar graph to compare the K_i of wild type and mutant proteins: R119H, R119S, R119Q and R119A; with respect to both GSH (blue) and bromoacetate (orange) substrates.

3.2.4 A Comparison of Kinetic Parameters of Wildtype versus Mutant Enzymes

The R119A, R119S, R119Q and R119H GstB mutants were created via site-directed mutagenesis by substituting arginine (R) at position 119 of GstB. Arginine-119 was found to form part of the H-site and is within 7Å of the GSH binding site.[14] The residue was proposed to dictate the binding of electrophilic substrates at the H-site.

The kinetic parameters suggest that the replacement of R119 with amino acid residues bearing different sizes, charges and polarity may have affected the binding of bromoacetate at the H-site. The replacement of the polar arginine residue with the non-polar alanine residue to form R119A, was observed to have a negative effect on the binding of bromoacetate at the H-site of GstB. The presence of the nonpolar residue at the substrate binding pocket may have created a hydrophobic environment discouraging the binding of negatively charged bromoacetate. A drop in the kinetic parameters of R119H, suggests that the size of the residue at position 119 of GstB, may also have played a role in the binding of bromoacetate. The imidazole ring of histidine being bulky may have created less space in the binding site obstructing the bromoacetate binding. The R119Q mutant, also experienced a decline in kinetic parameters compared to the wildtype GstB. The replacement of the positively charged residue of arginine with the uncharged glutamine residue at position 119 may have contributed to a decline in the binding of bromoacetate at the H-site. The behavior of these mutants indicates that the binding of bromoacetate is affected by the positive charge of the residue at position 119 of GstB polypeptide chain. Since GstB binds two substates, the effect caused by low binding of bromoacetate to the enzyme's binding pocket was also propagated to GSH.

CHAPTER 4: CONCLUSION

In summary, GSTs are important enzymes in the detoxication of xenobiotics as they have been found to be capable of catalyzing the conjugation of GSH to electrophilic substrates.[9] Because of this, an intensive study of the enzyme can offer insights into its use in environmental remediation.

The project examined four GstB mutants, created via site-directed mutagenesis, where arginine-119 was substituted with alanine, serine, glutamine, and histidine to form R119A, R119S, R119Q, and R119H mutants, respectively. A comparison of the turnover number (k_{cat}), the catalytic efficiency (k_{cat}/K_M) as well as the Michaelis constant K_M, revealed the significance of amino acid residue at position 119 in the binding of bromoacetate at the H-site. Replacement of the arginine with amino acid of different size, charge, and polarity decreased the activity of GstB towards bromoacetate compared to the wild type. Since GstB is a two-substrate enzyme, the effect of the mutation was also observed on the second substate, GSH.

Future work will involve the validation of the L114F and L114F/R119A mutations and the characterization of the newly created GstB mutants. Direct spectrophotometric assay will be performed and the reaction of GSH and CDNB will be monitored by measuring absorbance at 340 nm. The four mutants R119A, R119S, R119Q and R119H will be tested to establish their pH and temperature stability profiles.

REFERENCE

1. Briggs, D.; Environmental pollution and the global burden of disease. *Br. Med. Bull.* **2003**, 68 (1) 1–24
2. Murk, A. J.; Boudewijn, T. J.; Menninger, P. L.; Bosveld, A. T.; Rossaert, G.; Ysebaert, T.; Meire, P.; Dirksen, S. Effects of polyhalogenated aromatic hydrocarbons and related contaminants on common tern reproduction: integration of biological, biochemical, and chemical data. *Arch Environ Contam Toxicol* .**1996**, 31 (1), 128–140.
3. Vidali, M. Bioremediation. An overview. *Pure Appl. Chem*.**2001**.73, (7) 3.
4. Niti, C.; Sunita, S.; Kamlesh, K. Bioremediation: An emerging Technology for remediation of pesticides. *Res J Chem Environ*. **2013**, 17: 88-105.
5. Azubuike, C.C.; Chikere, C. B.; & Okpokwasili, G. C. Bioremediation techniques-classification based on site of application: principles, advantages, limitations, and prospects. *World J. Microbiol. Biotechnol*. **2016**, 32(11), 180.
6. Foreman, H. J.; Rinna, A.; Zhang, H. Glutathione: Overview of its Protective Roles, Measurement, and Synthesis. *Mol. Aspects Med*. **2009**, 30 (1-2), 1-12.
7. Armstrong, R. N.; Graminski, G. F.; Kubo, Y. Spectroscopic and Kinetic Evidence for the Thiolate Anion of Glutathione at the Active Site of Glutathione S-Transferase. *Biochemistry* **1989**, 28, 3562-3568.
8. Allocati, N.; Federici, L.; Masulli, M.; Di Illio, C. Glutathione Transferases in Bacteria. *FEBS J*. **2009**, 276, 58-75.
9. Desai, K. K; Miller, B; Recruitment of genes and enzymes conferring resistance to the nonnatural toxin bromoacetate. *PNAS* **2010** (42),17968-17973.

10. Booth, J.; Boyland, E.; Sims, P. An Enzyme from Rat Liver Catalyzing Conjugations with Glutathione. *Biochem. J.* **1961**, 79, 516-524. 22.

11. Al-Kassab, S.; Boyland, E.; Williams, K. An enzyme from rat liver catalysing conjugations with glutathione. Replacement of nitro groups. *Biochem. J.* **1963**. 87(1), 4–9.

12. Sheehan, D.; Meade G.; Foley, V.M; Dowd, C.A. Structure, function, and evolution of glutathione transferases: implications for classification of non-mammalian members of an ancient enzyme superfamily. *Biochem J.* **2001** 15;360,1-16.

13. Rossjohn, J.; Polekhina, G.; Feil, S. C.; Allocati, N.; Masulli, M.; Di Ilio, C.; Parker, M. W. A Mixed Disulfide Bond in Bacterial Glutathione Transferase: Functional and Evolutionary Implications. *Structure* **1998**, 15, 721–734

14. Chrysostomou, C., Quandt, E. M., Marshall, N. M., Stone, E., & Georgiou, G. An alternate pathway of arsenate resistance in *E. coli* mediated by the glutathione S-transferase GstB. *ACS Chem. Biol.* **2015**.10(3), 875–882.

15. McGuinness, M.; Mazurkiewic; Brennan, E. and Dowling, D. Dechlorination of pesticides by a specific bacterial glutathione S-transferase, BphKLB400: potential for bioremediation. *Eng Life Sci.* **2007**, 7, 611–615.

16. Riveron, J. M.;Yunta, C.; Ibrahim, S. S.; Djouaka, R.; Irving, H.; Menze, B. D.; Ismail, H. M.; Hemingway, J.; Ranson, H.; Albert, A.; & Wondji, C. S. A single mutation in the GSTe2 gene allows tracking of metabolically based insecticide resistance in a major malaria vector. *Genome Biol*. **2014**., 15(2), R27.

17. Wang ,Y.; Qiu, L.; Ranson, H.; Lumjuan, N.; Hemingway, J.; Setzer ,W.N.; Meehan, E.J.; Chen, L. Structure of an insect epsilon class glutathione S-transferase from the

malaria vector Anopheles gambiae provides an explanation for the high DDT-detoxifying activity. *J. Struct. Biol.* **2008,** 164(2) 228-235.

18. Moore, J. Tuning the Substrate Specificity of the Glutathione Transferase GstB from *Escherichia coli* via Site-directed Mutagenesis. M.S. Thesis, Youngstown State University, Youngstown, OH, **2017**.
19. Aboagye, C. Biochemical Characterization of Glutathione Transferase YliJ from *Escherichia coli.* M.S. Thesis, Youngstown State University, Youngstown, OH, **2015**.
20. Madej, T.; Lanczycki, C.J.; Zhang, D.; Thiessen, P.A.; Geer, R.C.; Marchler-Bauer, A.; Bryant, S.H. " MMDB and VAST+: tracking structural similarities between macromolecular complexes. *Nucleic Acids Res*. **2014,** 42, 297-303.
21. Armstrong, R. N.; Structure, Catalytic Mechanism, and Evolution of the Glutathione Transferases. *Chem. Res. Toxicol*. **1997**, 10, 2-18.
22. Pearson, WR. Phylogenies of glutathione transferase families. *Methods Enzymol.* **2005**; 401:186-204.
23. Mashiyama, S. T.; Malabanan, M. M.; Akiva, E.; Bhosle, R.; Branch, M. C.; Hillerich, B.; Jagessar, K.; Kim, J.; Patskovsky, Y.; Seidel, R. D.; Stead, M.; Toro, R.; Vetting, M. W.; Almo, S. C.; Armstrong, R. N.; Babbitt, P. C. Large- scale Determination of Sequence, Structure, and Function Relationships in Cytosolic Glutathione Transferases across the Biosphere. *PLoS Biol*. **2015**, 12, 1-19.
24. Kanai,T.; Takahashi, K.; Inoue, H. Three Distinct-Type Glutathione *S*-Transferases from *Escherichia coli* Important for Defense against Oxidative Stress. *J Biochem*. ***2006***, 140, 703–711.

25. Wadington, M. C.; Ladner, J. E.; Stourman, N. V.; Harp, J. M.; & Armstrong, R. N. Analysis of the structure and function of *YfcG* from *Escherichia coli* reveals an efficient and unique disulfide bond reductase. *Biochemistry* **2009**, 48(28), 6559–6561.
26. Wang, J; Youkharibache, P; Zhang, D.; Lanczycki, C. J; Geer, R. C, Madej, T, Phan, L.; Ward, M, Lu S,; Marchler, G. H,.;Wang Y, Bryant SH, Geer LY, Marchler-Bauer A. iCn3D, a Web-based 3D Viewer for Sharing 1D/2D/3D Representations of Biomolecular Structures. *Bioinformatics*. **2020**, 36(1), 131-135.
27. Rasko, D.A.; Rosovitz, M.J.; Myers, G.S.; Mongodin, E.F.; Fricke, W.F; Gajer, P.; Crabtree,J.; Sebaihia, M.; Thomson, N.R.; Chaudhuri, R.; Henderson, I.R.; Sperandio, V.; Ravel. J. The pangenome structure of *Escherichia coli*: comparative genomic analysis of *E. coli* commensal and pathogenic isolates. *J Bacteriol.* **2008**, 190 (20), 6881-93.
28. Burns, C.; Geraghty, R.; Neville, C.; Murphy, A.; Kavanagh, K.; Doyle, S. Identification, cloning, and functional expression of three glutathione transferase genes from *Aspergillus fumigatus*. *Fungal Genet. Biol.* **2005**, 42 (4), 319–327.
29. Holliday, G. L.; Mitchell, J. B.; Thornton, J. M. Understanding the functional roles of amino acid residues in enzyme catalysis. *J Mol Biol.* **2009**, 390 (3), 560–577.
30. Combes, B.; Stakelum, G. S. A Liver Enzyme that Conjugates Sulfobromophthalein sodium with Glutathione. *J. Clin. Invest*. 1961, 40 (6), 981- 988.